sustainability

MDPI

Article

Efficient Production of Wild and Non-Edible *Brassica juncea* (L.) Czern. Seed Oil into High-Quality Biodiesel via Novel, Green and Recyclable $NiSO_4$ Nano-Catalyst

Maryam Tanveer Akhtar [1], Mushtaq Ahmad [2], Maliha Asma [1], Mamoona Munir [2,3], Muhammad Zafar [2], Shazia Sultana [2], M. A. Mujtaba [4,*], Abdullah Mohamed [5] and Md Abul Kalam [6]

1 Department of Environmental Science, International Islamic University, Islamabad 44000, Pakistan
2 Plant Biodiesel Lab, Department of Plant Sciences, Quaid-i-Azam University, Islamabad 45320, Pakistan
3 Department of Botany, Rawalpindi Women University, Rawalpindi 46300, Pakistan
4 Department of Mechanical Engineering, University of Engineering and Technology, New Campus Lahore, Lahore 54890, Pakistan
5 Research Centre, Future University in Egypt, New Cairo 11835, Egypt
6 Faculty of Engineering and IT, University of Technology, Sydney 2007, Australia
* Correspondence: m.mujtaba@uet.edu.pk

Highlights:

- *Brassica juncea* (L.) Czern. seeds contain 30% oil content and 0.43 mg KOH/g FFA content.
- Ni-TG nano-catalyst was synthesized through a wet impregnation route.
- The Ni-TG nano-catalyst has a crystalline size of 39.29 nm with a semispherical and ovoid shape.
- 0.3 wt% catalyst concentration, 6:1 methanol to oil ratio at 90 °C for 120 min yielded 93% of *Brassica juncea* (L.) Czern. biodiesel.

Abstract: In the current study, a novel green nano-catalyst from Tragacanth gum (TG) was synthesized and used for sustainable biodiesel production from *Brassica juncea* (L.) Czern. seed oil. *Brassica juncea* (L.) Czern contains 30% oil on dry basis and free fatty acid content of 0.43 mg KOH/g. Physiochemical characterization of a newly synthesized nano-catalyst was performed by X-ray Diffraction (XRD), Scanning Electron Microscopy (SEM), Energy Dispersive X-ray (EDX), Transmission Electron Microscopy (TEM), and Fourier Transform Infrared Spectroscopy (FT-IR) analysis. The XRD results showed an average crystalline size of 39.29 nm. TEM analysis showed the cluster form of $NiSO_4$ nanoparticles with a size range from 30–50.5 nm. SEM analysis of the catalyst showed semispherical and ovoid shapes with surface agglomeration. The synthesized catalyst was recovered and re-used in four repeated transesterification cycles. Maximum biodiesel yield (93%) was accomplished at 6:1 methanol to oil molar ratio, catalyst concentration of 0.3 wt%, at 90 °C for 120 min at 600 rpm using Response Surface Methodology (RSM) coupled with central composite design (CCD). *Brassica juncea* (L.) Czern. biodiesel was characterized by Thin Layer Chromatography (TLC), FT-IR, Nuclear Magnetic Resonance (NMR) (^1H, ^{13}C), and Gas Chromatography-Mass Spectroscopy (GCMS) analytical techniques. The major fatty acid methyl esters were 16-Octadecenoic acid and 9-Octadecenoic acid methyl ester. The fuel properties, i.e., flash point (97 °C), density (825 kg/m^3 at 40 °C), kinematic viscosity (4.66 mm^2/s), pour point (–10 °C), cloud point (–14 °C), sulfur content (66 wt.%), and total acid number (182 mg KOH/g) were according to the International biodiesel standards. The reaction kinetic parameters were determined, and all the reactions followed Pseudo first-order kinetics. It was concluded that non-edible *Brassica juncea* (L.) Czern. seed oil is one of the sustainable candidates for the future biofuel industry using a cleaner, reusable, and highly active Ni-modified TG nano-catalyst.

Keywords: non-edible seed oil; biodiesel; green nano-catalyst; response surface methodology; kinetic studies; catalyst reusability

check for updates

Citation: Akhtar, M.T.; Ahmad, M.; Asma, M.; Munir, M.; Zafar, M.; Sultana, S.; Mujtaba, M.A.; Mohamed, A.; Kalam, M.A. Efficient Production of Wild and Non-Edible *Brassica juncea* (L.) Czern. Seed Oil into High-Quality Biodiesel via Novel, Green and Recyclable $NiSO_4$ Nano-Catalyst. *Sustainability* **2022**, *14*, 10188. https://doi.org/10.3390/su141610188

Academic Editor: Ioanna Ntaikou

Received: 29 June 2022
Accepted: 8 August 2022
Published: 17 August 2022

1. Introduction

Fossil fuels, i.e., coal, oil, and natural gas, are dominant energy resources that are limited, expensive, and cannot be replaced rapidly at a human time scale [1]. They require thousands of years to get restocked. Fossil fuels depletion and several other environmental concerns, i.e., climate change, global warming, ozone depletion, and volatility, have been associated with the use of fossil fuels. Global warming (increase in temperature) also causes land use changes and high accumulation of GHGs in the atmosphere, disturbing the nature balance [2]. The identification of energy needs and environmental problems shifts the researcher's attention toward renewable, clean, and sustainable energy sources [3]. The best renewable energy carriers are biofuels which exhibit some intriguing characteristics [4]. Biodiesel is widely accepted nowadays as a transportation alternative fuel [5]. Biodiesel consists of mono alkyl esters commonly derived from animal fats or vegetable oils [6]. It is non-toxic, renewable, biodegradable, has high flash points, too low emission of particulate matter (PM), CO_2, SO_2, and unburnt hydrocarbons [7]. Additionally, biodiesel mixed with diesel fuel in the vehicle can unusually decrease air pollution [8]. Due to these characteristics, biodiesel has been widely accepted nowadays as a transportation alternative to fuels.

Fuel quality can be increased by the addition of certain micron-sized particles as an additive. Other modifications include changes in engine design, such as changes of combustion chamber and injector nozzle geometry. It is a significant way to neutralize fuels with high viscosity [9]. Nanoparticles exhibit distinguishing features, i.e., magnetic, thermal, electrical, and optical properties. The addition of a small amount (a few grams) of nanoparticles in the base fuel increases the combustion and reduces exhaust emissions such as CO_2, SO_x, NO_X, CO and smoke emissions [10]. The authors of [11] studied Lemon Peel Oil (LPO) blended with diesel with three proportions of LPO10, LPO20, and LPO30. The best results were obtained from LPO20 in terms of engine characteristics. Oxygenated fuel additive, i.e., Diethyl ether (DEE), was added in LPO20 in different amounts of 5% and 10%. It was found that LPO 20 DEE 10 showed improvement in engine performance and reduced harmful exhaust emissions. Recently, research has mainly focused on the exploration and utilization of various non-edible feedstocks for bioenergy [12]. Feedstock selection mainly depends upon its availability in a specific area and it also contributes to biodiesel production cost. The main reason for the high cost of biodiesel production is the use of virgin oil as feedstock which accounts for 70–90% of total production costs [4,13], causing a major hindrance to its commercialization.

A non-edible feedstock is preferred in order to overcome the expenses of biodiesel production and compete with the strong food versus fuel debate. Different non-edible feedstocks have been used for biodiesel production, including *Silybum marianum*, *Hevea btobaccos*, *Eruca sativa*, *Nicotiana tabaccum*, *Azadharacta indica*, *Pongamia pinnata* [14], *Sterculia foetida* [15], *Capparis spinosa* [16], spent frying oil [17], chicken fat [18], sulfonated tea waste [19], *Prunus armeniaca* (L.) [20], and so forth. *Brassica juncea* (L.) Czern., commonly known as "Chinese mustard" or "brown mustard" and "oriental mustard", belongs to the family Brassicaceae. It is an annual herb, native to Eastern and Southern Asia that grows erectly up to 30–90 cm and is sometimes 200 cm tall, glabrous above, and sparsely hairy below with simple hairs. The lower leaves are predominantly stalked, and the upper leaves are acute, oblong to linear. The flowers are golden yellow, the pedicel is 5–8 mm, and racemes are lax. The petals are yellow in color and adjacent to a shorter and longer stamen, whereas the four free sepals are 1–1.5 mm broad, 4–6 mm in length, oblong, glabrous, and yellowish, with an apex that is obtuse or rounded. The stamens are 4–6:5–8 mm, often curved, and obtuse with an apex. The siliquae are 25–50 mm in length, linear, broad subterraneous, with a 5–10 mm long narrowed seedless beak, the valve having a prominent yellowish midrib, glabrous, and 1 mm in diameter. The style has a short stigma and is 1.5–2.5 mm in length. The seeds are 10–20 in each locule, globose, 1 mm in diameter, and reddish brown in color. It is wild in central Asia and extensively cultivated across the world. It can produce 1000–2000 kg seeds per hectare [21] and has an oil content of 30–38%.

It grows well in irrigated and rain-fed areas of Pakistan. Due to the wild and non-edible nature, the price of *Brassica juncea* (L.) Czern. seeds are low; it is therefore preferably used as a sustainable bioenergy source for cost-effective methyl ester production at an industrial scale.

Several biodiesel production methods show that biodiesel has massive potential for energy applications [22]. These technologies include direct blending, micro-emulsions, pyrolysis, and transesterification [23]. Crude vegetable oil has a high viscosity and cannot be used directly in a diesel engine. Therefore, it can be diluted or directly mixed with a diesel engine to improve its viscosity. The specific amount of crude oil that is mixed with diesel fuel is usually 1:10–2:10 oil to petroleum diesel fuel; however, direct use of crude vegetable oil or a blended ratio of more than the given value, high FFA content, and acid value makes it unsuccessful for both direct and indirect diesel engines [24]. Micro emulsification or co-solvency is a process in which crude vegetable oil is mixed with alcohol (emulsifying agent). Although, this process decreases the viscosity of crude vegetable oil and causes incomplete combustion and accumulation of carbon in the engine, and irregular injection needle sticking [23]. Thermal cracking or pyrolysis is the breakdown of complex molecules of crude oil (triglycerides) into a less complicated structures by adding thermal energy. The fuel obtained from this process possess similar characteristics to petroleum diesel and is also suitable for diesel engine. The disadvantages associated with pyrolysis are the poor oxygenated value of biodiesel, sophisticated technology requirements, and higher production costs. It also contains a higher amount of sulfur and moisture content [25].

Transesterification, also known as "alcoholysis", is the easiest, cost-effective, and most widely used method for biodiesel production by producing good quality fuel with the same physicochemical properties as conventional diesel fuel [26]. In this process, three moles of triglycerides, which are an active constituent of fats and oils, react with one mole of alcohol, particularly methanol, to produce biodiesel [27]. Transesterification reaction proceeds in the presence of a catalyst or without a catalyst by using alcohols. Methanol and triglycerides are immiscible due to poor surface contact and slow down the transesterification process. The catalyst is a substance that speeds up the chemical reaction without itself being consumed during the reaction. It makes the production process easier, faster, and more efficient. The use of catalysts in the reaction improves the surface contact between methanol and crude oil (triglycerides) and increases the rate of reaction.

Generally, homogeneous or heterogeneous (organic or inorganic) catalysts are used in the biodiesel production process [28]. Homogeneous catalysts (NaOH and KOH) have certain disadvantages, i.e., reactor corrosion, soap formation, and emulsification, which can cause difficulty in the separation of the catalyst from the product (biodiesel) and reduce the yield of methyl esters [29]. However, heterogeneous catalysts are non-corrosive, can easily separate from the reaction mixture, and also have the ability to recycle and reuse. The problems related to the use of heterogeneous catalysts are the leaching of catalytic active sites, long reaction time, and high reaction temperature that raises the value of the nano-catalyst for biodiesel synthesis. The nano-catalyst can perform functions on the atomic scale by exhibiting high catalytic activity, non-corrosiveness, high selectivity, nano dimension, and porous morphology [30]. The transesterification process mediated by the nano-catalyst has several advantages, i.e., fast and easy separation of the catalyst from the product mixture and an increase in the rate of mixing with the reactants in a short reaction time [31].

Commonly, two methods are used for nano-catalyst synthesis; the first is the chemical method and the second is through the green method. In the chemical synthesis method, different chemicals are used with strong reagents and solvents which increases eco-toxicological concerns, while the green synthesis method is safe and environmentally friendly as it involves the use of enzymes, microbes, and plant exudates [32]. Plant exudates are basic substrates, selected for nanoparticle synthesis because they contain stabilizers, natural reducing agents, surfactants, and environment-friendly properties. Surfactants increase the interaction among triglycerides and methanol and significantly increase the

biodiesel production rate [33]. A large number of plant metabolites act as a catalyst and enhance the reaction rate [34]. Nano-catalysts synthesized through green methods can be used further in organic transformation reactions. Tree gums have fascinating properties such as being biocompatible, eco-friendly, safe, and a cheap plant-based polysaccharide. TG is the exudate from Astragalus gummifer and is a naturally occurring polysaccharide. It contains Bassorin (water insoluble) but swells when added to water and Tragacanth, which is water soluble [35]. Moreover, this natural polysaccharide consists of (1 → 2), (1 → 3), and (1 → 5)-linked *L*-arabinose with (1 → 3) and (1 → 6)-linked galactose. In addition, the major constituent of TG is *α-D*-galacturonan substituted in *O-3* with *β-D*-xylose [36].

In the present research study, novel, non-edible *Brassica juncea* (L.) Czern. seeds were utilized as the cheapest feedstock for biodiesel synthesis. A recoverable and reusable green phyto-nano-catalyst (TG modified Ni) was synthesized by the wet impregnation route. Single-step transesterification was used for biodiesel synthesis from *Brassica juncea* oil in the presence of the green phyto-nano-catalyst. The physiochemical properties of the synthesized nano-catalyst and biodiesel were evaluated by different analytical techniques. The developed method may provide a new step in the production of clean fuels and green chemistry technologies. The response surface methodology was explored to identify the parameter's influence on biodiesel production. Finally, biodiesel fuel properties were determined and compared with international standards.

2. Materials and Methods

2.1. Materials

The seeds of the *Brassica juncea* (L.) Czern. plant were collected through various field trips across Pakistan and compared with conserved samplings from Herbarium of Pakistan, followed by a comparison with the Flora of Pakistan. The collected seeds were cleaned properly to eradicate dust, then oven dried at 55 °C. These dried seeds were crushed with the help of a grinder into a fine powder. TG was purchased from the local market in Rawalpindi, Pakistan. Nickel sulfate ($NiSO_4$), methanol (99% purity), and n-hexane were used. All the used chemicals were of analytical grade, purchased from Sigma Aldrich (Islamabad, Pakistan), and used without purification.

2.2. Oil Extraction

A known amount (15 g) of ground seeds was fed into a thimble equipped with a reflux condenser and a round bottom flask was poured with solvent (n-hexane 200 mL). The flask was placed at the end of the Soxhlet apparatus which was also equipped with a tightly fixed condenser at the end. The entire setup was heated at a temperature range from 60 °C for 5–6 h and *B. juncea* oil was collected in a round bottom flask. After the completion of the process, the wet sample was oven dried for 24 h to evaporate the solvent and measure the difference between the initial and final sample weights to calculate the oil content of *Brassica juncea* seeds. The following Equation (1) was used to calculate the yield of *Brassica juncea* seeds oil (BJSO) [30].

$$\text{BJSO Yield } (\%) = \frac{Mass\ of\ oil\ produce}{Mass\ of\ sample\ used} \times 100 \quad (1)$$

2.3. Analysis of Free Fatty Acids Content of Extracted Oil

FFA content of BJSO was determined through the aqueous acid-base titration (sample and blank) method [29]. In the blank titration process, 0.025 molar KOH solution was poured into a conical flask comprising three drops of phenolphthalein as indicator solution and 10 mL isopropanol [37]. The solution was titrated until its color turned pink and then the value was recorded. Whereas in the sample titration, 1 mL of BJSO and 9 mL of isopropanol were mixed and titrated against KOH solution. The titration was stopped

when its color changed to pink. The following Equation (2) was used to determine the FFA content of BJSO [16].

$$\text{Acid no (mg KOH/g)} = \frac{(\text{A} - \text{B}) \times \text{M}}{\text{W}} \quad (2)$$

Here, A and B are volumes of titrant used for sample and blank titration, M is the volume of titrant solution, and W is the sample weight (in g).

2.4. Catalyst Synthesis and Characterization

The $NiSO_4$ nano-catalyst using TG was synthesized by the in situ wet impregnation method with some modifications [37]. First, TG support was prepared by mixing a known amount (2 g) of TG into 500 mL distilled water at a 70 °C temperature. The mixture was continuously heated and refluxed until a clear solution was obtained. A metal precursor solution was prepared, i.e., 10 g $NiSO_4$ was added to prepared Tragacanth gum solution (TGS) and refluxed for 7 h at 600 rpm. The resulting sample was filtered, oven dried at 110 °C, calcined at 500 °C for 3 h, and ground into fine powder for further characterization.

The structural properties of the TG-Ni green nano-catalyst were analyzed through XRD analysis with a D8 Advance BRUKER diffractometer using monochromatic Cu Kα with 1.54 Å at 45 kV and 40 mA. Sample scanning was performed in the range of 2^{θ} from 10–70° with a scan rate of 2°/min. The average particle size was calculated by the Debye–Scherer method as shown in Equation (3) [18].

$$\text{D} = \frac{K\lambda}{\beta \cos \theta} \quad (3)$$

where *K* represents the Scherer constant, λ denotes the X-ray wavelength, β stands for the height of the diffraction peak, and θ denotes the angle of diffraction. The SEM Model KYKY Em-6900 was used to determine the surface morphology of the prepared catalyst at accelerating voltage 2 kv using an electron microscope. Whereas the EDX (BRUKER) was performed to confirm the chemical composition of the prepared TG-Ni nano-catalyst. The catalyst was layered with gold for 80 s in 30 s breaks before the measurement to evade the charging problem. The morphological aspect of the Ni-modified TG nano-catalyst was studied by using Transmission Electron Microscopy (TEM) (Jeol TEM) Model (JEM-200CX). The FT-IR (Derkin Elmer, Spectrum 65) technique was also used to examine the chemical structure of the prepared catalyst within the wavelength range of 500–4000 cm^{-1}using the KBr technique.

2.5. Reflux Transesterification Process for Biodiesel Synthesis

A schematic and pictorial representation of the biodiesel synthesis is shown in Figure S1. The non-edible BJSO was converted into biodiesel through the reflux transesterification route. The TG-Ni green nano-catalyst and alcohol were mixed to perform the reaction in a glass reactor of 250 mL equipped with a reflux condenser to prevent methanol escape during the reaction and fixed on a hot plate with a magnetic stirrer. A cooling water recirculation system was also fitted with the system. A fixed volume of filtered BJSO was preheated at 55 °C and the desired amount of prepared TG-Ni catalyst was added in different oil to methanol ratios under constant temperature, catalyst loading, and stirring at 600 rpm for the appropriate time. The resulting reaction mixture contained methanol, glycerol, and biodiesel. The mixture was heated at 60 °C to evaporate the methanol and the remaining glycerol and the *Brassica juncea* biodiesel (BJBD) were separated with the help of a separating funnel. The upper layer contained methyl esters, and the lower layer had glycerin. The resultant biodiesel yield was calculated using Equation (4) [29].

$$\text{Yield of BJBD (\%)} = \frac{Mass\ of\ biodiesel\ produced\ (g)}{Mass\ of\ oil\ used\ (g)} \times 100 \quad (4)$$

2.6. Biodiesel Characterization

BJBD analysis was performed by thin layer chromatography (TLC). A silica-coated aluminum plate, "chromatographic plate", was used. A small drop of crude oil and its corresponding methyl ester was applied to one side of the plate and placed vertically in a glass vial comprising a thin layer of developing solvent (acetic acid, n-hexane, and diethyl ether) with a ratio (8:1:30). The drops components dragged along the plate and reached the required point. After that, the chromatographic plate was removed, dried, and placed in an iodine chamber for staining. Fatty acid methyl esters and triglycerides molecules have differences in polarity and molecular mass, so they interact differently with the stationary phase [38]. The resultant spots of triglycerides and biodiesel were recognized through iodine vapor stains. The results obtained from TLC were calculated using the following equation [39].

$$R_f = \frac{Distance\ traveled\ by\ sample}{Distance\ traveled\ by\ solvent\ front} \quad (5)$$

R_f (retention factor) was used to identify and confirmed the conversion of triglycerides into fatty acid methyl ester (FAME) in this study. The R_f value of seed oil lies within the given range of (0.20–0.35), and greater than (>0.60) confirms the synthesis of biodiesel.

The synthesized *BJBD* was also characterized by various analytical techniques. The chemical composition and functional groups present in the synthesized biodiesel were examined through FT-IR spectroscopy using DERKIN ELMER, Spectrum 65 in the range from 4000–500 cm^{-1}. Fifteen scans for biodiesel analysis were performed under 1 cm^{-1} resolution. The configuration of synthesized FAME was determined through GCMS with (GC-QP 2010) ultra by SHIMADZU with a column temperature of 130–300 °C at the rate of 80 °C/mi. Helium gas was induced with a flow rate of 1.44 mL per minute. The injector temperature was set at 130 °C while the detector temperature was 350 °C with a capillary column of 30–0.32 mm and 0.25 µm film thickness. The mass spectrometer scan range was 50–1000 m/z ratio with the Electron Impact (EI) ionization mode. The total program was protracted for 30 min. NMR analysis was performed to analyze the distribution of total methyl esters. Both ^{1}H NMR and ^{13}C NMR analyses of biodiesel were performed to monitor the transesterification reaction. Avan CE 300 MHz spectrometer fortified with 5-mm Brad Band Observe (BBO) probes at 7.05 T. Tetra methyl silane and deuterated chloroform were used as an internal standard and solvent, respectively. ^{1}H NMR and ^{13}C NMR spectra were verified with a 30° pulse duration and the recycle delay for ^{1}H NMR was recorded at 1.0 scans and 8 scans, while for ^{13}C NMR, the recycle delay of 1.89 scans and 160 scans. The biodiesel yield was quantified using Equation (6) [40].

$$C = 100 \times \frac{2A(Me)}{3A(CH2)} \quad (6)$$

where C is the % conversion of oil into biodiesel, Proton integration values (Methoxy and α-Methylene) are *A(Me)* and *A(CH2)*.

2.7. Experiment Design and Statistical Analysis by Response Surface Methodology

The effect of different parameters on the BJBD yield was analyzed by RSM coupled with CCD. The effect of various independent parameters at different levels on the result (dependent variable) was examined by analysis of variance (ANOVA) [41]. In a current research study, the effect of four independent variables on biodiesel yield from *BJSO* is was examined by the response surface methodology (Design Expert 13, Stat-Ease Inc., Minneapolis, MN, USA) based on CCD. Thirty experimental runs were completed to study four independent variables, i.e., (A) catalyst concentration (0.1–0.5 wt %), (B) reaction temperature (30–150 °C), (C) methanol to oil molar ratio (2:1–10:1), and (D) reaction time (60–360 min). The interaction between each numeric factor and its response was positioned at the quadratic response surface, and the mathematical relationship among independent

variables (A, B, C, D) and the predicted response value (Y) was described by the second-order polynomial model Equation (7) [42].

$$Y = \beta_0 + \sum_{i-1}^{k} \beta_i X_i + \sum_{i-1}^{k} \beta_{ii} X_i 2 + \sum_{i-1,\, i<j}^{k} \beta_{ij} X_i X_j + e \quad (7)$$

Here, the response is represented by (Y) which is (conversion %), β_i(linear), β_{ii}(quadratic), and β_{ij}(interactive) coefficients. X_i and X_j are coded process variables (A, B, C, D). Statistical analysis of the RSM model was performed to examine the ANOVA, whereas the graphical analysis of data was carried out by Design Expert 13 software (Stat- Ease Inc., Minneapolis, MN, USA) [43].

2.8. Catalyst Reusability

Nano-catalyst reusability is also an important aspect to make it cheaper and preferable over homogeneous and heterogeneous catalysts. The reusability test was carried out under optimized conditions, i.e., methanol to oil ratio 6:1, catalyst concentration 0.3 wt% at 75 °C temperature, and 2 h reaction time. After the phase separation process of biodiesel, the left-over catalyst was recovered by centrifugation of the reaction mixture at 3000 rpm for 10 min. Afterwards, the recovered catalyst was washed with hot distilled water, n-hexane solvent, and oven dried at 60 °C overnight followed by calcination at 500 °C for 3 h before use for the next cycle. The reaction cycle stopped when a significant decrease in biodiesel yield was observed. It is necessary to wash the catalyst to remove the attached molecules of reaction media at the catalyst surface [44].

2.9. Determination of Biodiesel Properties

Physico-chemical properties of BJBD were examined. These include density at 40 °C (ASTM D 6751), kinematic viscosity at 40 °C, flash point (°C) (ASTM D 93), sulfur content (wt.%) (ASTM D 4294), and acid value (mg KOH/g) (ASTM D 974) and then compared with the American Standard and Testing Materials (ASTM D 6751), ASTM D-951 which is the international biodiesel standard of America and European Union [15].

2.10. Reaction Kinetics of Brassica juncea (L.) Czern. Seeds Oil into Biodiesel

The reaction kinetics was used to examine the relationship between time and temperature and its dependence on optimized reaction conditions for the transesterification process. The reaction follows the first order reaction as the product biodiesel (methyl esters) formation is studied as a time function. A reversible reaction is assumed to follow various reaction orders concerning product formation. The product at different time intervals is used to find the rate constant. The kinetics equation is given as:

$$\frac{d[P]}{d[t]} = k[P] \quad (8)$$

Here, k: rate constant (min^{-1}) and it depends on time and temperature, P (synthesized methyl esters in terms of yield %), and t: reaction time (min). The plot ln [P] versus ln [dP]/[dt] at different intervals of time and temperature was found to be linear where the rate constant was determined from the intercept and slope. The activation energy is computed through the Arrhenius equation and is essential for the transesterification process. The relationship between reaction rate (constant) and temperature is defined by the Arrhenius Equation (9) as given below.

$$\ln k = -\frac{Ea}{Rt} + C \quad (9)$$

Whereas, k represents the rate constant of reaction, Ea is activation energy (kJ), t is for absolute temperature, and R is for gas constant [45].

3. Results and Discussion

3.1. Oil and Free Fatty Acids Content of B. juncea (L.) Czern. Seeds

Seed collection at the appropriate time, pretreatment process, and the solvent used are important factors that help in determining the oil content [46]. The determined oil content based on the dry biomass of *B. juncea* seeds is 30%, which proves the viability of this novel feedstock for biodiesel production at an industrial scale. Before dispensation of BJSO into biodiesel, the FFA content of the seeds was also determined. The recorded FFA content of BJSO was 0.43 mg KOH/g.

3.2. Catalyst Characterization

The morphology and size of the prepared Ni-TG nano-catalyst were analyzed by using different characterization techniques. The XRD technique was used for investigating the size, elemental composition, and crystal structure of the nano-catalyst. The XRD pattern was calculated by basal reflection peaks d (001) as shown in Figure 1. The detected diffraction peaks were compared with the Joint Committee on Powder Diffraction Standards (JCPDS), The sharp diffraction peaks confirm the good crystallinity of the synthesized nano-catalyst. The database diffraction points observed at angular positions of 2 θ value at 20.71 (110), 22.78 (020), 25.08 (111), 26.82 (021), 35.23 (200), 38.71 (130), 45.40 (202), 51.31 (222), 55.20 (042), and 66.80 (331) were in accordance with the standard database (JCPDS file No. 01-072-1195). The diffractogram of the catalyst sample showed the d value (basal spacing) appearing at 4.30, 3.92, 3.56, 3.34, 2.55,2.33,1.99, 1.78, 1.66, and 1.39Å, respectively. The average crystalline size was calculated using the Debye–Scherrer formula (Equation (3)) and was 39.29 nm. In the present study, the calculated average particle size confirmed that the $NiSO_4$ particles synthesized from the green method are in nano size. In [47], the synthesized and characterized NiO green nano-catalyst was used. The intense diffraction peaks were observed at 2 θ (37.42, 43.4, and 62.89) which are assigned to (111), (200), and (220) planes. The crystallite size of NiO nanoparticles is 8.15 nm and it was predicted from the (200) plane. In the present study, the dominant peak is also observed at the (200) plane due to the occurrence of several phytochemicals in Tragacanth gum exudate which plays a significant role in the reducing and capping agent to the synthesize green nano-catalyst [48]. X-ray diffraction results of the $NiSO_4$ modified TG nano-catalyst were found in accordance with SEM.

The surface morphology of the Ni-TG nano-catalyst was studied by SEM. The SEM micrographs of the Ni-TG nano-catalyst at different magnifications are shown in Figure 2 with different morphology after calcination at 500 °C. The physical properties of $NiSO_4$ were influenced by the addition of the surfactant (TG). The synthesized nano-catalyst exhibited a semispherical and ovoid shape. Nano-catalysts with varying sizes were observed in the present analysis. An agglomeration observed at some places on the surface was due to TG support. The micrographs recorded at different magnifications confirm the presence of micro pores among those micro grains [40,49]. SEM micrographs confirms the uniform distribution of Ni at the micrometer scale. The surface morphology of the NiO nano-catalyst mentioned in the literature is spherical and cubic in shape. However, in comparison, the present study has shown a slightly different shape of the synthesized Ni-TG nano-catalyst (spherical and ovoid) with microporous morphology that further enhances the catalytic activity of the nano-catalyst for biodiesel production.

The elemental composition of the synthesized novel green Ni-TG nano-catalyst was studied via EDX analysis as shown in Figure 3. The EDX spectra exhibited the high peaks of Ni, S, and O which confirms the synthesis of the $NiSO_4$ nano-catalyst. The overall percentage of these high peaks are Ni (34.07 wt%), S (10.36 wt%), and O (17.96 wt%) in the synthesized catalyst. The semi-quantitative elemental composition of the synthesized nano-catalyst shows a C peak, which is probably from the active compounds of Tragacanth gum exudates involved in the synthesis and capping of the nanoparticles. Results of the EDX spectrum confirm the purity of the synthesized green nano-catalyst and are suggested for biodiesel production.

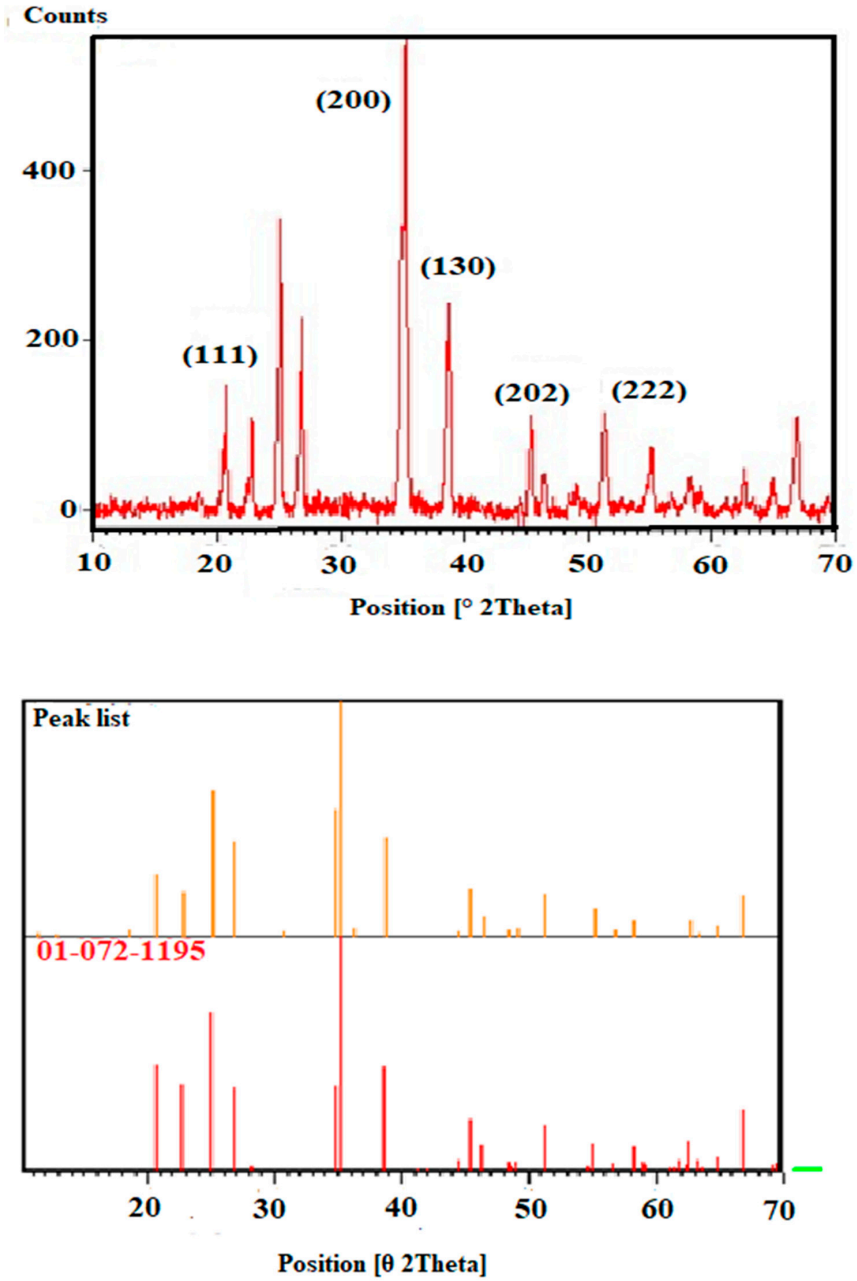

Figure 1. XRD graph of the Ni modified Tragacanth gum nano-catalyst matched with the JCPDS Card.

The morphological and structural characteristics of the $NiSO_4$ modified TG nano-catalyst are shown in Figure 4 which reveals the presence of monodisperse particles. TEM analysis is based on the transition of electrons from a substance. There are some light and dark parts in the image, usually, the light part shows much denser parts of material and less transition of electrons, and contrariwise, the dark part represents less dense material and better electron passage. These micrographs clearly show that the $NiSO_4$ nanoparticles are present in cluster forms on the surface of the support (TG) and the size of the nanoparticle is in the 30–50.5 nm range. The particle size determined from the TEM micrograph is similar to the size reported by applying the Debye–Scherrer equation to the XRD patterns. In [50], the authors used *Anogeissus latifolia* gum for the synthesis of Palladium nanoparticles and TEM characterization was performed. The results indicated the spherical shape of particles with sizes ranging from 2.3 to 7.5 nm and from the corresponding diameter, the average obtained particle size was 1.6–4.8. The capping of organic material (gum exudates)

makes the catalyst more stable. The spaces among the monocrystalline are observed in the mesoporous form.

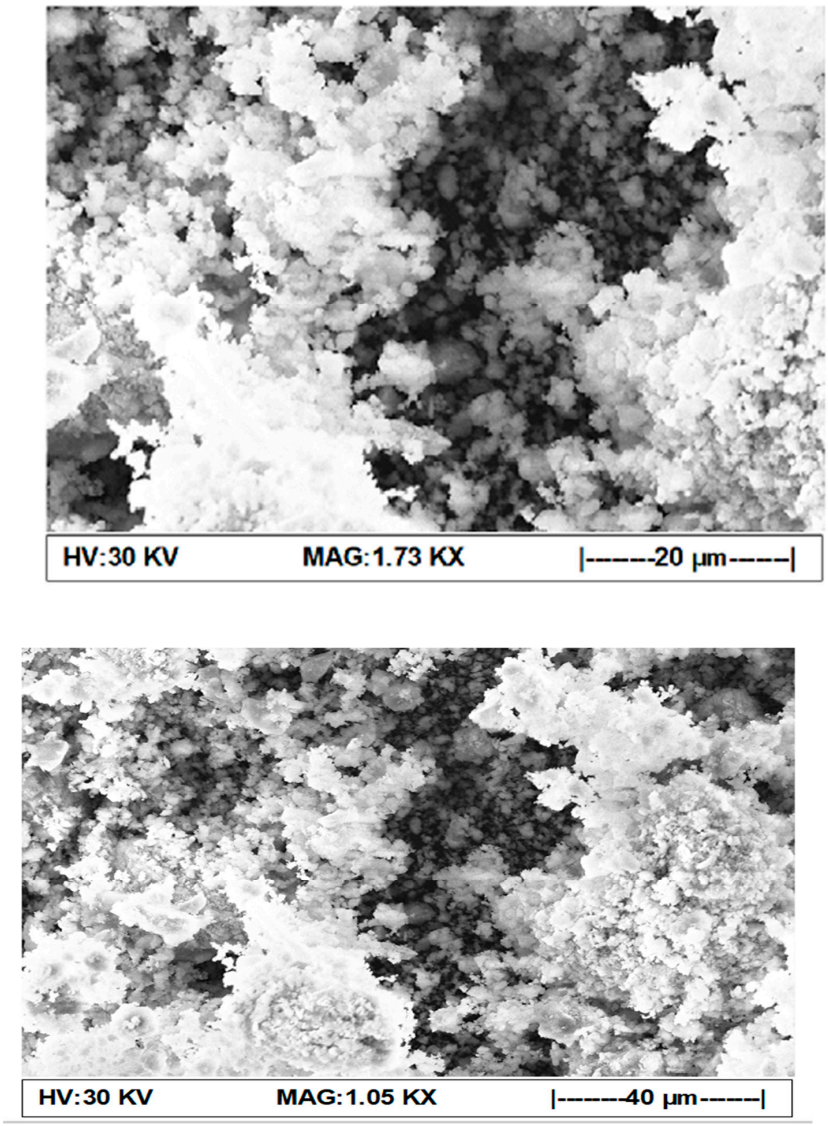

Figure 2. SEM Micrographs of Ni modified Tragacanth gum nano-catalyst at different resolutions.

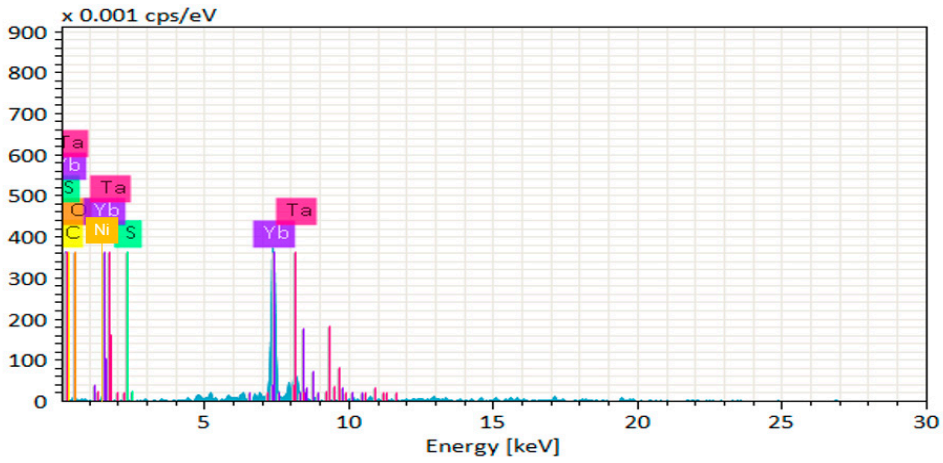

Figure 3. EDX of Ni modified Tragacanth gum nano-catalyst.

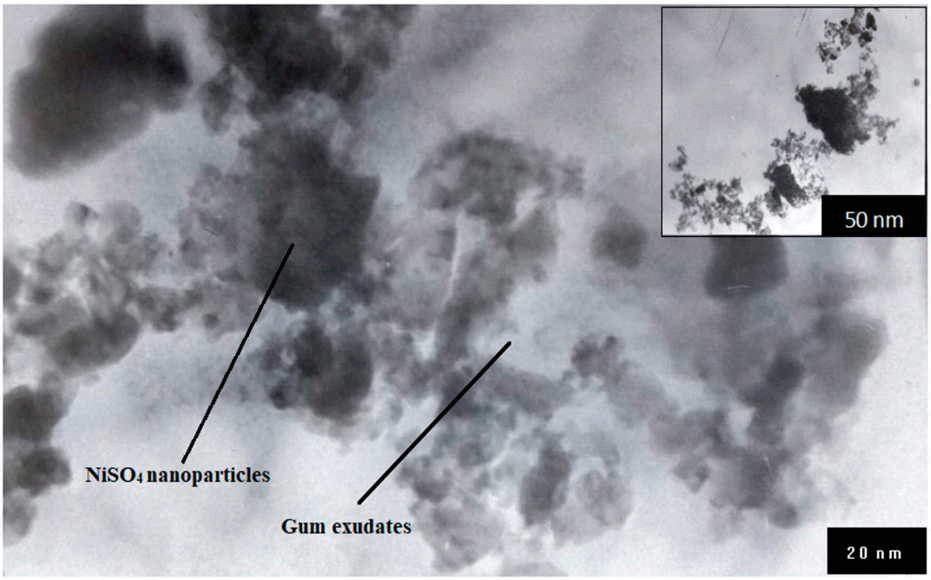

Figure 4. TEM Micrograph of Ni modified Tragacanth gum nano-catalyst.

Different functional groups present in Ni-TG nano-catalyst were analyzed from the FT-IR spectra (Figure 5). The spectrum shows different peaks with a broad band in the region of 4000 cm^{-1}–450 cm^{-1}. The presence of the absorption band at 2937.79 cm^{-1} is owed to weak -OH stretching vibrations of adsorbed phenolic compounds with nickel metal ion. The peak that appeared at 2840.59 cm^{-1} represents weak -CHO stretching. At peak 1674.74 cm^{-1}, the absorption band was detected with -OH bending vibrations and aromatic rings, comparable to previously described work in the literature [51]. Two strong intensive peaks were observed at 1111.19 cm^{-1} and 1013.21 cm^{-1} which exhibited the sulfate group symmetric and asymmetric vibrations of S-O and S=O. The peak that appeared at 559.87 cm^{-1} was related to Ni-O. In [52], the authors also found absorption peaks similar to the present study. Both the phenolic and aromatic compounds as a capping were also observed in the previous literature [53]. So, overall FTIR results conclude that the nano-catalyst synthesized using plant gum exudates is capable of acting as a reducing and stabilizing agent.

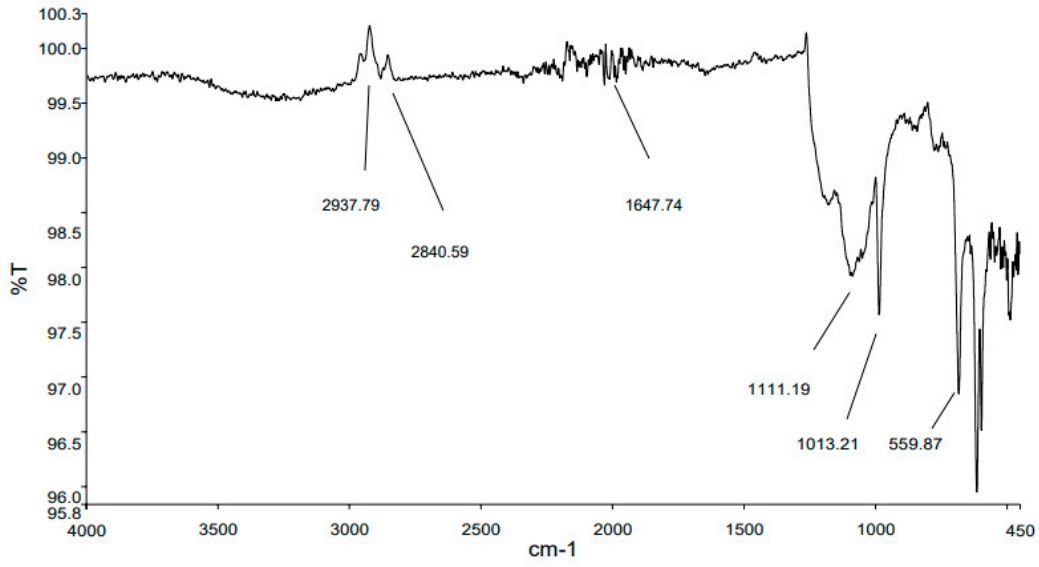

Figure 5. FT-IR Spectra of Ni modified TG nano-catalyst.

3.3. Response Surface Methodology for Optimization of Synthesized Biodiesel

Reflux transesterification of *BJSO* was carried out in the presence of the Ni-modified TG nano-catalyst. The four-factor independent variables (Table 1), i.e., catalyst concentration (0.1–0.4 wt. %), (B) reaction temperature (30–150 °C), (C) molar ratio of methanol to oil (2:1–10:1), and (D) reaction time (60–360 min) was used in the transesterification process for optimization of BJBD. The relationship among input variables and output response (Y) is evaluated by the coded model Equation (7) as shown.

$$Y = +86.55 + 0.1667\ A + 0.8333\ B + 3.44\ C + 0.6396\ D - 2.56\ AB - 0.1875\ AC - 3.56\ AD - 1.56\ BC + 1.06\ BD - 1.56\ CD - 2.48\ A^2 - 26.48\ B^2 - 7.98\ C^2 + 7.58\ D^2$$

Table 1. Experimental and predicted data for biodiesel yield of *Brassica juncea* L. Czern seed oil using central composite design.

Runs	Catalyst Concentration (wt. %)	Reaction Temperature (°C)	Methanol to Oil Molar Ratio	Reaction Time (min)	Experimental Yield (%)	Predicted Yield (%)
1	0.2	120	4.1	135	51.55	50.45
2	0.3	150	6.1	210	75.88	75.21
3	0.4	120	8.1	135	80.65	81.74
4	0.2	120	8.1	135	59.32	60.22
5	0.3	90	6.1	60	46.21	45.49
6	0.2	120	8.1	285	60.68	61.23
7	0.1	90	6.1	210	58.37	58.30
8	0.2	60	8.1	135	45.25	45.21
9	0.4	60	4.1	285	54.37	53.58
10	0.3	90	6.1	120	93.00	93.31
11	0.2	60	8.1	285	49.88	48.67
12	0.2	120	4.1	285	49.66	49.00
13	0.4	120	4.1	135	61.29	60.98
14	0.3	90	6.1	120	92.48	92.31
15	0.2	60	4.1	360	45.11	46.65
16	0.3	90	6.1	135	92.94	93.00
17	0.3	90	2.1	120	41.97	42.79
18	0.3	90	6.1	210	91.74	91.76
19	0.4	120	8.1	120	88.31	88.71
20	0.4	60	8.1	285	68.77	67.70
21	0.2	60	4.1	285	50.48	51.00
22	0.3	90	6.1	120	93.01	93.28
23	0.1	120	4.1	360	65.31	66.18
24	0.1	90	6.1	60	86.18	85.84
25	0.3	90	6.1	120	59.63	58.67
26	0.4	60	8.1	120	57.46	57.44
27	0.3	90	6.1	210	93.00	92.81
28	0.3	30	6.1	60	51.82	51.19
29	0.3	90	10.1	60	66.11	65.17
30	0.4	60	4.1	120	47.62	48.16

ANOVA results (Table 2) measure the fitness of the model, the parameters show the model F-value (223.95) is significant with a *p*-value (8.5), whereas the F-value corresponding to lack of fit (4.71) with a *p*-value (0.05) is insignificant with pure error, indicating that the model is fit with experimental (trial) data. The determination of coefficient value R^2 = 0.995% confirms the model variability 99.5 %. The difference between the predicted R^2 value (0.990) and the Adjusted R^2 value (0.974) is less than 2, confirming the good correlation with regression polynomial. Furthermore, the adequate precision value (42.34) is greater than 4, indicating the suitability of this model to navigate the design in space, thus predicting the biodiesel yield [54]. Additionally, in Figure 6, the straight line shows

a close agreement between the experimental and predicted biodiesel yield. The 3D graph in Figure 7A–F depicts the interactive effect of four independent variables on the transesterification process for biodiesel production.

Table 2. ANOVA for response surface quadratic model.

Source	Sum of Squares	Df	Mean Square	F-Value	*p*-Value	
Model	9355.739078	14	668.267077	223.9565557	8.52948×10^{-15}	Significant
A-Catalyst Concentration	1168.591704	1	1168.59170	391.6305053	3.67734×10^{-12}	
B-Reaction Temperature	887.5584375	1	887.5584375	297.4477383	2.66636×10^{-11}	
C-Oil to Methanol Ratio	739.3710042	1	739.3710042	247.7856372	9.80758×10^{-11}	
D-Reaction Time	181.7751042	1	181.7751042	60.91834783	1.16531×10^{-6}	
AB	84.87015625	1	84.87015625	28.44256216	8.36177×10^{-5}	
AC	145.6245563	1	145.6245563	48.80320333	4.3819×10^{-6}	
AD	25.67955625	1	25.67955625	8.605997762	0.010270002	
BC	87.28230625	1	87.28230625	29.25094674	7.25258×10^{-5}	
BD	17.87175625	1	17.87175625	5.989367293	0.027184179	
CD	7.16900625	1	7.16900625	2.40255131	0.141976017	
A^2	2582.357295	1	2582.357295	865.4262123	1.1103×10^{-14}	
B^2	3505.566673	1	3505.566673	1174.821661	1.15787×10^{-15}	
C^2	4757.985331	1	4757.985331	1594.54512	1.19913×10^{-16}	
D^2	3153.558452	1	3153.558452	1056.85303	2.5353×10^{-15}	
Residual	44.75870833	15	2.983913889			
Lack of Fit	40.469175	10	4.0469175	4.7172002	0.050379608	Not significant
Pure Error	4.289533333	5	0.857906667			
Cor Total	9400.497787	29	**R^2**	0.995238687		
Std. Dev.	1.727401		**Adjusted R^2**	0.990794796		
C.V.%	2.616376		**Predicted R^2**	0.974546095		
			Adeq Precision	42.34321891		

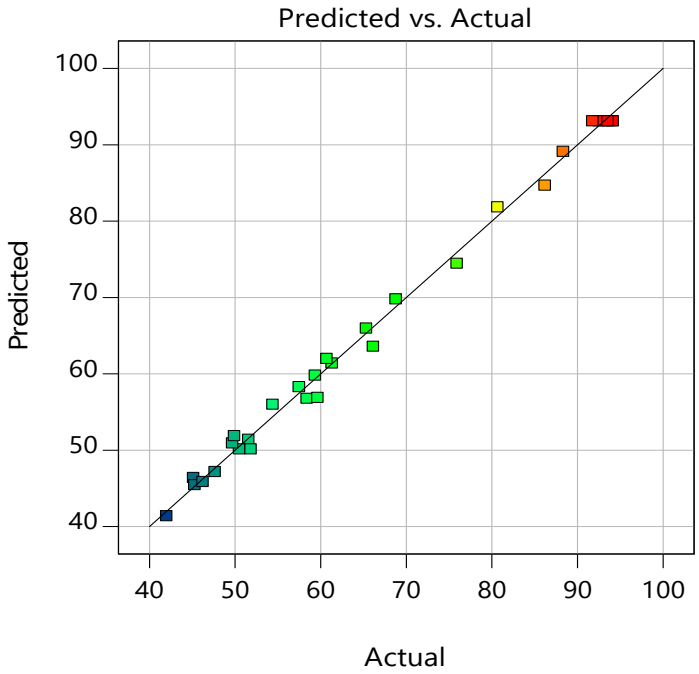

Figure 6. Predicted yield vs. actual yield of *Brassica juncea* (L.) Czern. biodiesel.

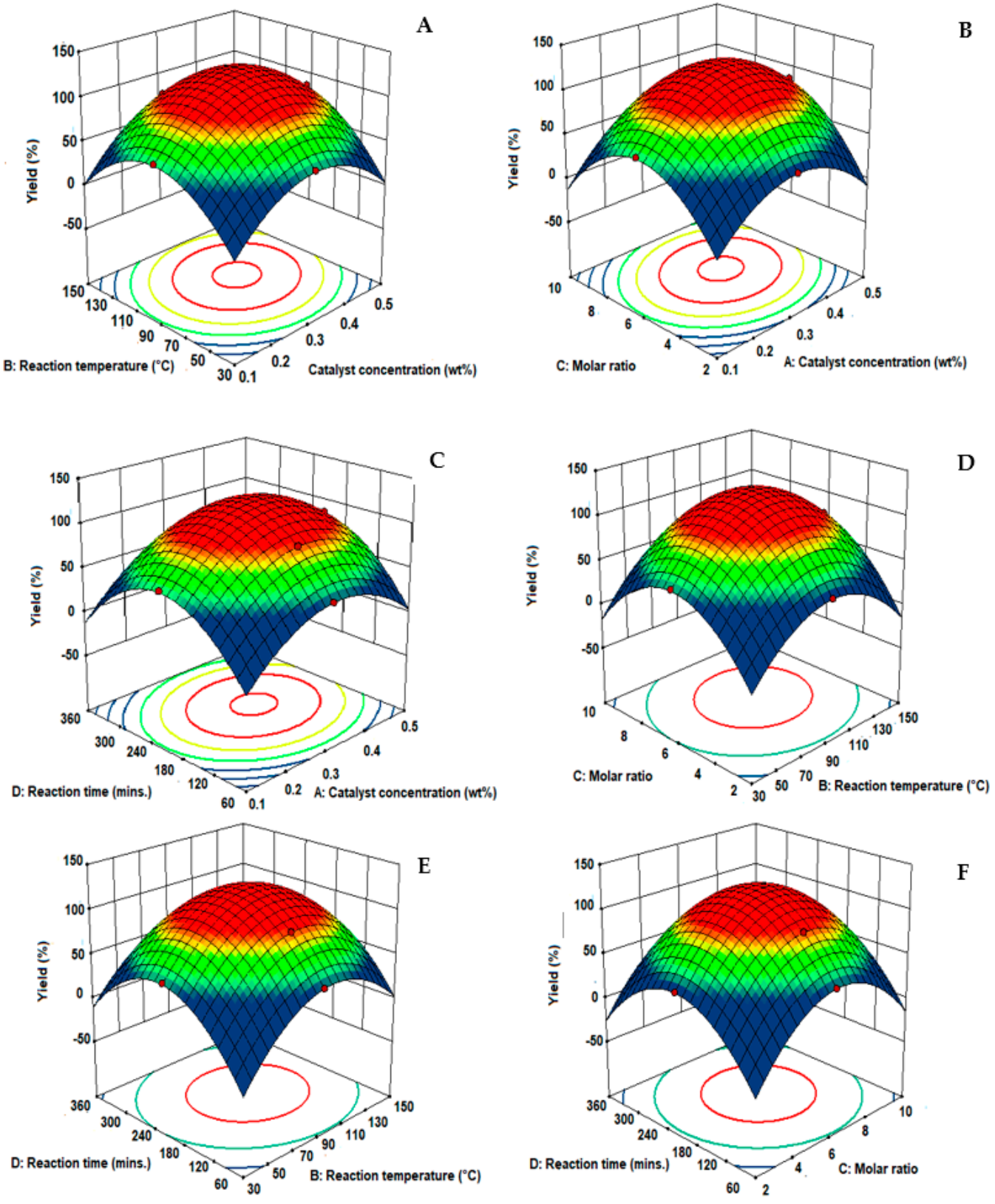

Figure 7. 3D Graphs (**A**–**F**) presenting the influence of various reaction parameters on *Brassica juncea* (L.) Czern. biodiesel yield.

3.3.1. Collaborative Effect of Catalyst Concentration and Reaction Temperature

The three-dimensional (3D) graph in Figure 7A depicts the collaborative effect of the catalyst concentration and reaction temperature on the final biodiesel yield where the reaction time and oil to methanol ratio were kept constant. The highest yield (93%) was attained at a 90 °C reaction temperature and 0.3 wt% catalyst concentration (Run 10) (Table 1). It is clearly depicted in Figure 7A that as the catalyst concentration increases from 0.1–0.3 wt.% and the reaction temperature from 30 °C–90 °C, the yield of biodiesel also increased up to 93%. However, a further increase in the catalyst concentration >0.3 wt.% and the reaction temperature >90 °C leads to a decrease in the biodiesel yield up to 61.29% (Run 13) (Table 1). As the catalyst concentration increased above the threshold limit, the reaction mixture becomes more viscous, resulting in a drop in the yield of biodiesel at 54.37% (Run 9). Meanwhile, the increase in temperature above the threshold limit reduces its interaction with the catalyst due to higher volatility and decreases the biodiesel yield by 75.88% [55]. These results are in line with the findings of [54]. The ANOVA results show that the collaborative effect of the catalyst concentration and the reaction temperature is insignificant due to the *p*-value (8.36) > 0.05.

3.3.2. Collaborative Effect of Catalyst Concentration and Methanol to Oil Molar Ratio

The collaborative effect of the catalyst concentration and methanol to oil molar ratio on biodiesel yield is shown in Figure 7B. The 3D graphs show the highest biodiesel yield (93 %) was attained with a 6:1 methanol to oil molar ratio and catalyst concentration 0.3 wt% (Run 16). Both parameters play an important role in maximizing the biodiesel yield. The molar ratio is one of the significant parameters that determines the yield of biodiesel. Stoichiometrically, in the transesterification reaction, 3 mol of biodiesel and 1 mole of glycerol are produced from 3 mol of methanol and 1 mole of oil. The transesterification process is double-sided, so a supplementary amount of methanol is required for the forwarding reaction. The maximum catalyst concentration of 0.4 wt% resulted in a decreased biodiesel yield of 61.29 %. However, the increase in the methanol to oil molar ratio 8:1 and catalyst concentration 0.4 wt.% of the biodiesel yield decreased to 57.46% (Run 26). This is due to the reversible reaction which combines fatty acid methyl esters with glycerol and forms monoglycerides and a decreased the biodiesel yield [56]. These results are similar to the reported literature [37] where the supplementary amount of methanol favors the backward reaction and reduces the yield of biodiesel. In the present study, the 1:4 oil to methanol molar ratio and 0.1 wt% catalyst concentration were found deficient in biodiesel synthesis and a decrease in biodiesel yield up to 65.31% was observed at Run 23. However, higher amounts of methanol cause difficulties in the separation of glycerol from biodiesel and decreased the biodiesel yield. Thus, ANOVA results concluded that the interactive impact of these parameters is insignificant $p = 4.38$, which is >0.05. A similar insignificant correlation between the catalyst concentration and oil to methanol ratio was observed in ANOVA results presented in the literature [57]

3.3.3. Collaborative Effect of Catalyst Concentration and Reaction Time

Figure 7C presents the interactive impact of the catalyst concentration and reaction temperature on *Brassica juncea* (L.) Czern. biodiesel yield, whereas the other two parameters remain constant. The 3D surface plot shows that an increase in the catalyst concentration of 0.3 wt.% and reaction time up to 120 min produced a 93% biodiesel yield (Run 10) due to equilibrium. However, beyond these optimized reaction conditions, such as 0.4 wt% catalyst concentration and 285 min reaction time, there is an abrupt drop in the yield of biodiesel (68.77 %) (Run 20) due to the shifting of the reaction in a backward direction and altering the product back into the reactants. Furthermore, if the catalyst concentration remains the same, i.e., 0.3 wt%, and decreased the reaction time to 60 min, it results in a decreased biodiesel yield (46.21 %) (Run 05). The shorter reaction time inhibits the completion of the reaction [58]. The comparable results observed in the literature at lower reaction time and catalyst concentration decreased the biodiesel yield [59]. These study

parameters are significant with p-value = 0.01 < 0.05 for the transesterification process. The significant correlation in the present study is found similar to the correlation observed in a previous study [60].

3.3.4. Collaborative Effect of Reaction Temperature and Methanol to Oil Molar Ratio

The combined effect of the reaction temperature and methanol to oil molar ratio on biodiesel yield is shown in Figure 7D. The highest biodiesel yield of 93% was attained at a 90 °C reaction temperature and 6 mL methanol (Run 10) (Table 1). However, above the threshold limit at 150 °C, a significant decline in a biodiesel yield of 49.66% was observed (Run 12). Although, a higher reaction temperature provides more kinetic energy to the reactant molecules to increase the yield of biodiesel in a shorter reaction time. The increase in temperature above the threshold limits increases the glycerin saponification and reduced the amount of biodiesel yield. However, a decrease in the reaction temperature of 60 °C resulted in a decrease in the biodiesel yields of 45.11 %. This is due to the immiscibility of oil, catalyst, and methanol at low temperatures. Whereas, the highest methanol to oil molar ratio 10:1 resulted in a decline in the biodiesel yield up to 66.11 %. This is due to that, after the threshold limit, the evaporation of methanol results in decreasing the biodiesel yield [61]. This was also observed in the work of of [62]. Thus, the ANOVA results concluded that the collaborative effect of the reaction temperature and oil to methanol molar ratio is insignificant due to its p-value (p = 7.25) > 0.05.

3.3.5. Collaborative Effect of Reaction Temperature and Reaction Time

The collaborative effect of the reaction time and reaction temperature on biodiesel yield is presented in Figure 7E. A substantial increase in the yield of biodiesel (93% Run 22) was observed at a 90 °C temperature and 120 min reaction time. Further increase in the reaction temperature (150 °C) and reaction time (210 min) decreased the biodiesel yield (75.88 %) due to the saponification. According to the Arrhenius equation, an increase in reaction temperature increases the reaction rate gradually and also the yield of biodiesel. After that, the considerable decrease in the biodiesel yield resulted, due to the endothermic nature of the transesterification process. Moreover, the long reaction process causes evaporation of methanol and drops the biodiesel yield, meanwhile the short reaction time inhibited the interaction of oil and the catalyst resulting in the insignificant conversion of oil into FAME. A minimum biodiesel yield (47.62%) was observed at 60 °C. These results match the findings present in the following literature [37]. Whereas, high reaction temperature and time eased the hydrolysis process to produce acid along the polarity of methanol and decreased the yield of biodiesel. Therefore, ANOVA results depict the significant collaborative effect of the reaction temperature and time on biodiesel yield with a p-value = 0.02 (<0.05).

3.3.6. Collaborative Effect of Methanol to Oil Molar Ratio and Reaction Time

The combined effect of the methanol to oil molar ratio and reaction time on the final yield of biodiesel is shown in Figure 7F while other parameters, i.e., reaction temperature 90 °C and catalyst concentration 0.3 wt%, remain constant. The highest biodiesel yield (93% Run 10) was obtained at a 6:1 molar ratio of methanol to oil and 120 min reaction time, attributed to increased interaction between oil and methanol. However, in (Run 14) the obtained biodiesel yield was 86.18% with a 6:1 methanol to oil molar ratio and 60 min reaction time. The reason behind this is the short reaction time; the reactants did not reach the equilibrium stage and resulted in the incomplete conversion of triglycerides into biodiesel. The reported literature work also confirmed the decline in *Jatropha Curcas* biodiesel yield at a short reaction time and oil to methanol molar ratio. A minimum methyl ester yield of 41.97% was observed at a 2:1 methanol to oil molar ratio whereas at a minimum reaction time of 60 min, the obtained biodiesel yield is 51.82 %. Moreover, in the present study, the biodiesel yield also decreased at a 10:1 methanol to oil molar ratio and 360 min reaction time, where the dilution effect of oil reduced the biodiesel yield and

higher reaction time lead to a reverse transesterification reaction and decreased biodiesel yield. The authors in [37] also observed a similar pattern in their research study. ANOVA results show that the interactive impact of these two parameters is insignificant with (p = 0.14) > 0.05.

3.4. Biodiesel Characterization

3.4.1. Fourier Transform Infrared Spectroscopy Analysis of *Brassica juncea* (L.) Czern. Biodiesel

Figure 8A represents the FTIR spectra of *Brassica juncea* (L.) Czern. oil and Figure 8B represents the spectra of *BJBD*. FTIR graphs showed not much difference in the IR spectra of *B. juncea* oil and BJBD; however, in some regions, differences in band intensity and absorbance frequency of both spectrums were observed. The fingerprint region ranging from 1500–900 cm^{-1} is the main region that allows chemical differentiation between oil and biodiesel [38]. In oil, spectra functional groups appeared at 3308.15 cm^{-1}, 2946.56 cm^{-1}, 2834.63 cm^{-1}, and 1652.01 cm^{-1}, representing (sp^2 C-H), (sp^3 C-H), (C=O stretch), respectively. A strong peak detected at 1744.52 cm^{-1} confirms the ester formation in Figure 8B. The peak observed at 1436.58 cm^{-1} shows asymmetric stretching vibrations of -CH_3. Some other changes were also observed within the ester control peak area during the transesterification of *B. juncea* oil into biodiesel. The stretching of O-CH_3 represented the transmittance at 1114.26 cm^{-1} of biodiesel. Alkanes group stretching was observed at 594.66 cm^{-1}. In [63], the authors synthesized biodiesel from algae (*E. compressa*) in the presence of a chicken waste derived catalyst. The peaks observed at 1745 cm^{-1}, 1445 cm^{-1}, and 722 cm^{-1} correspond to C=O stretching, an asymmetric stretch of -CH_3- and CH_2 bending. The peaks noted in the present study are similar to the reported work in the literature. The changes observed in biodiesel spectra are due to methyl ester moiety which is absent in the crude *Brassica juncea* oil spectra. Therefore, the resultant biodiesel attained after the transesterification reaction of *Brassica juncea* (L.) Czern. oil through the Ni-modified TG nano-catalyst was confirmed as biodiesel.

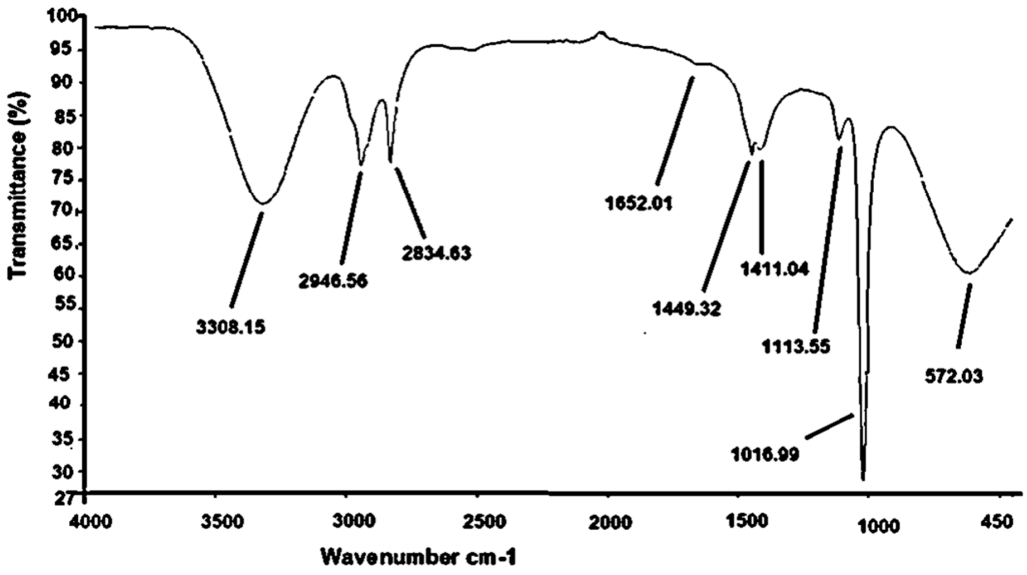

(**A**)

Figure 8. *Cont.*

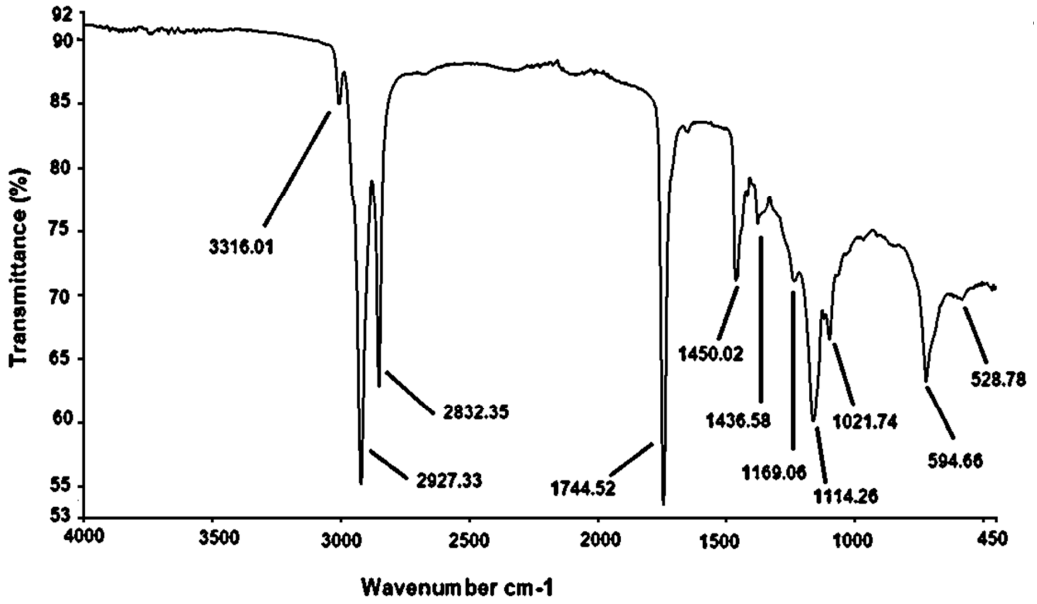

(**B**)

Figure 8. FT-IR spectrum of (**A**) *Brassica juncea* (L.) Czern. seed oil (**B**) *Brassica juncea* (L.) Czern. biodiesel.

3.4.2. Gas Chromatography Mass Spectroscopic Analysis

The quantitative analysis of methyl esters in biodiesel was conducted through GC-MS. It is a widely used and vastly suitable analytical technique to analyze the structure and composition of methyl esters present in biodiesel. The gas chromatogram spectrum of the Ni-TG catalyzed biodiesel showed seven major peaks in Figure S2. The individual peaks of the chromatogram were analyzed in the NIST mass spectra library 11. The saturated methyl esters fragmentation is: 16-Octadecenoic acid, methyl ester, Pentadecanoic acid, 14-methyl, methyl ester, Hexadecanoic acid, methyl ester, and 6-Octadecenoic acid, methyl ester. Whereas two unsaturated methyl esters are 9-Octadecenoic acid, methyl ester, and 8, 11, 14-Docosatrienoic acid, methyl ester. The observed base peaks of saturated and unsaturated fatty acid methyl esters are at m/z 28 and 68. The library match provides evidence that the abundantly present methyl esters in *Brassica juncea* (L.) Czern. biodiesel is 16-Octadecenoic acid methyl ester and 9-Octadecenoic acid methyl ester, which provides stability to synthesized biodiesel [64].

The primary determinant of a feedstock's suitability for biodiesel synthesis is its fatty acid methyl ester composition. From the library match, it is evident that abundantly present ester in the understudy *Brassica juncea* L. oil is octadecanoic acid methyl ester. This substance has a strong propensity to give biodiesel stability. Peroxidation and polymerization induced a greater level of unsaturation and reduced the methyl esters suitability [65]. A higher temperature in combustion engines accelerates peroxidation, which leads to engine clogging. Therefore, the feedstock with a higher concentration of polyunsaturated acids is not appropriate for biodiesel synthesis. Additionally, monounsaturated acids have little or no affinity to oxygen which causes peroxidation. The dominant methyl ester is the same as reported in the literature [16], thus confirming the suitability of the understudy seed oil as an efficient feedstock for the biodiesel industry.

3.4.3. Nuclear Magnetic Resonance Studies

^{1}H NMR Analysis

The *BJSO* and biodiesel were analyzed by ^{1}H NMR and ^{13}C NMR spectroscopy and their spectra are represented in Figure S3 (upper). The ^{1}H NMR spectra of *BJSO* showed triglycerides at 4.1–4.3 ppm and signals that appeared at 5.30–5.35 ppm confirm the presence

of olefinic protons (unsaturated hydrocarbons). Whereas, the ^{1}H NMR spectra of *BJBD* in Figure S3 (lower) shows the characteristic single peak at 5.4 ppm exposed methoxy protons (-OCH_3), which confirms the methyl esters formation. Additional peaks were at triplet of alpha methylene protons (α-CH_3) at 2.01–2.78 ppm, terminal methyl protons (-CH_3) at 0.84–0.88 ppm, (β-CH_2) at 1.24–1.98 ppm, (-CH_2-COO-) at 2.01–2.29 ppm, (-CH=CH-) at 5.30–5.33 ppm, respectively. Similar peak positions were observed by [37] and a major significant peak was observed at 3.76 ppm related to the methoxy group –OCH_3-. The results of ^{1}H NMR in the present study are in line with the reported work.

^{13}C NMR Analysis

Figure S4 presents the ^{13}C NMR spectrum of *B. juncea* oil and methyl esters. The characteristic signals appeared at 62.0 and 68.8 ppm in the ^{13}C NMR spectrum of oil, Figure S4 (upper), corresponded to the -O-CH_2- and -O-CH- and represents the presence of glycerides functional groups. However, in biodiesel spectra, Figure S4 (lower), the new peak appeared at 51.4 ppm is related to -OCH_3 methoxy carbon and the signal appears at 173.28 ppm is the characteristic of the ester carbonyl group (-COOR). The signals shown at 27.20 ppm (-CH_2-) in ethylene carbons of long carbon chains, 76.67 ppm (-C-O), and 127.87 ppm, specify (-CH=CH-) the degree of unsaturation in methyl esters of *Brassica juncea* (L.) Czern. [16]. By using Equation (5), the total conversion of *BJSO* into *BJBD* is 93% which is very close to the (90.3%) yield obtained practically. The lower practical yield as compared to the calculated biodiesel yield through NMR can be improved by giving more settling time to the product or using a more effective separation process like centrifugation [66]. The literature study also shows the signal of the ester group carbon is located at 60 ppm and 174 ppm [67]. Therefore, the ^{13}C NMR results of the present study confirm the successful conversion of triglycerides into their corresponding methyl esters.

3.5. Catalyst Reusability Test

In this study, the reusability of the synthesized Ni-TG nano-catalyst was tested at the optimal experimental conditions of reflux transesterification, i.e., catalyst concentration 3 wt%, molar ratio of methanol to oil 6:1, for 2 h at 75 °C. From the reaction products, the used catalyst was recovered and reprocessed for the next reaction cycle under the same conditions. The results in Figure 9 show that the regenerated catalyst activity does not change for the first three cycles with a maximum 90% yield of biodiesel. Thereafter, the catalyst poisoning prevents the catalytic sites from chemical reaction and decreases the biodiesel yield. The results of the present study are also comparable with the literature [39]. It confirms that catalyst structure changed after three cycles. The irregular and smaller particle size of the fresh catalyst agglomerated and gradually got bigger and reduced catalytic activity. Another reason behind that is the deposition of unreacted triglycerides on the catalyst surface [68].

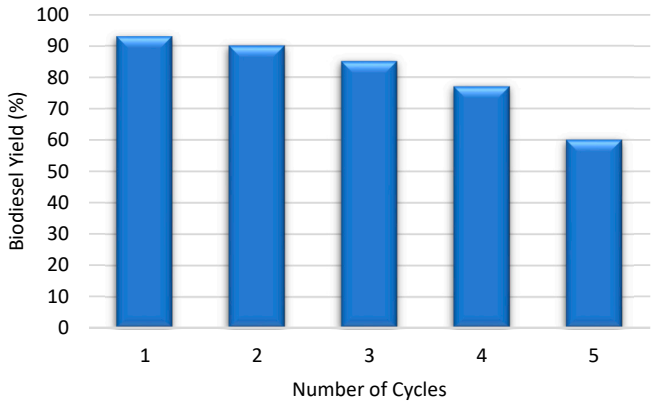

Figure 9. Catalyst reusability cycle analysis at optimal reaction parameters.

3.6. Physicochemical Characterization of Synthesized Biodiesel

The physicochemical properties of the synthesized *Brassica juncea* (L.) Czern. biodiesel under optimal reaction conditions was compared with international biodiesel standards. The measured fuel properties are represented in Table 3. The color of *BJBD* is on visual 2 in accordance with international standards. The ignition temperature of the fuel is called the flash point. The high flash point of fuel makes it safer during the handling, transportation, and storage process [37]. The flash point (97 °C) of synthesized biodiesel is to some extent higher than the given value of ASTM D-93 but in accordance with EN 14214. Pour and cloud points are the cold flow properties that are important for analyzing biodiesel quality. Biodiesel color changes to milky when the surrounding temperature decreases due to the formation of crystal nuclei that stop the fluid pouring. So, the cloud point is that at which crystal formation takes place and the minimum temperature at which the fuel becomes solidified and looses its flow characteristic is known as the pour point. The pour point (−10 °C) and cloud point (−14 °C) are higher to some extent than the international standards and can be upgraded by using some commercially available additives and antioxidants. Density directly affects fuel efficiency, biodiesel density gives insight intothe fatty acids and transparency of biodiesel, which ultimately depends on the number of carbon atoms. Density strongly linked to viscosity means higher fuel density causes viscosity problems in the engine [14]. The density of *Brassica juncea* (L.) Czern. methyl esters were 0.825 (kg/m^3 at 40 °C), which is within the prescribed limit of international standards and ensures that the synthesized methyl esters could be the best alternate option to use in a diesel engine without affecting the diesel locomotives and environment. During the combustion process, kinematic viscosity plays an important role. The higher viscosity may create hindrances during combustion [15]. The kinematic viscosity of BJBD is 4.66 mm^2/s, which shows an equivalence to international standards. Fuel with sulfur contents is more effective for engine operations and the environment [61]. Sulfur content in BJBD of 0.0066 wt.% is within the limit defined by international standards. The acid number is another important property related to the free fatty acids amount in fuel. A high acid value causes corrosion in the internal engine combustion and affects its function. In the present study, the acid value of synthesized biodiesel is 0.182 mg KOH/g, which within international standards (ASTM-D6751, ASTM-D951, and EN 14214).

Table 3. Comparison of *Brassica juncea* (L.) Czern. fuel properties with international biodiesel standards.

Properties	Methods	BJBD ALM-B100	HSD ASTM D-951	ASTM D-6751	EN-14214
Color	Visual	2	2.0	2	-
Flash point (°C)	ASTM D-93	97	60–80	≥93	≥120
Density (kg/m^3 at 40 °C)	ASTM D-1298	0.825	0.8343	≤120	≤120
K. Viscosity (mm^2/s at 40 °C)	ASTM D-445	4.66	4.223	1.9–6.0	3.4–5.0
Pour point (°C)	ASTM D-97	−10	-	−15–16	-
Cloud point (°C)	ASTM D-2500	−14	-	−3–12	-
Sulfur content (wt.%)	ASTM D-4294	0.00066	0.05	≤0.05	0.020
Total Acid No (mg KOH/gm)	ASTM D-974	0.182	0.8	≤0.5	≤0.5

3.7. Reaction Kinetics of Brassica juncea (L.) Czern. Biodiesel

The kinetic study of various reaction orders (zero order, first order, and second order) of transesterification was carried out at optimum reaction conditions, i.e., molar ratio of alcohol to oil 6:1, catalyst amount 0.3 wt%, reaction time 60–200 min, and in the temperature range of 60–90 °C as shown in Table 4. A study of reaction kinetics at various temperatures exposed that the reaction is a pseudo first-order reaction and well fitted with an experimental yield of biodiesel from triglycerides of *Brassica juncea* (L.) Czern. A good linear relation was observed between $-\ln(1 - x)$ and the reaction time at three different temperatures (60 °C, 70 °C, 80 °C, and 90 °C) as presented in Figure 10. The reaction order was found using Equation (8) of reaction kinetics.

Table 4. Calculated values of kinetic parameters for BJBD.

Temperature (°C)	k min^{-1}	R^2	E_a kJ
60	0.066	0.929	381.48
70	0.079	0.9428	
80	0.183	0.9524	
90	0.058	0.9798	

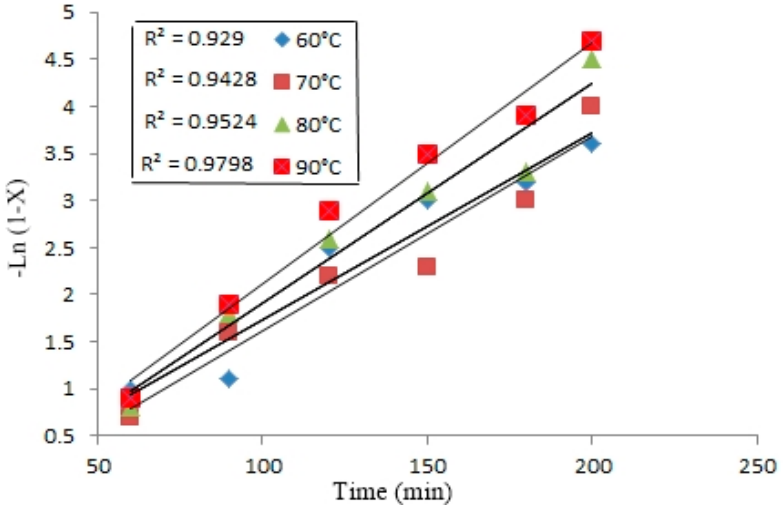

Figure 10. Plot of (pseudo first order reaction) −ln (1 − x) vs. time at various temperatures for BJBD.

Values of R^2 were calculated from plots of concentration vs. time and −ln(1 − x) vs. time at different reaction temperatures. The activation energy of transesterification reaction of *Brassica juncea* (L.) Czern. seed oil catalyzed by Tragacanth gum modified the Ni nano-catalyst and was calculated from the slope of the graph plotted between lnK and 1/T whose values are summarized in Table 4. The plots of lnK vs. 1/T slopes showed that the activation energy of the transesterification reaction was found to be 381.48 kJ. This investigation revealed that only a little of amount energy is required to convert triglycerides of *Brassica juncea* (L.) Czern. seed oil into methyl esters with the Ni-TG nano-catalyst. The activation energy in the current study was found lower as compared to previous findings of [15] and higher than the findings of [69].

4. Conclusions

This research work is confined to examine the potential of novel and non-edible *BJSO* for biodiesel production using a recyclable green Ni-modified TG nano-catalyst. *Brassica juncea* (L.) Czern. contains a high seed oil content (30%) and FFA content of 0.43 mg KOH/g, which confirms its suitability for biodiesel production. The synthesized green nano-catalyst shows significant catalytic activity during the reflux transesterification process for the conversion of BJSO into biodiesel. The maximum biodiesel yield (93%) was attained under optimized transesterification reaction parameters, i.e., methanol to oil ratio 6:1, catalyst concentration 0.3 wt%, 90 °C reaction temperature, reaction time 120 min, and 600 rpm stirring speed. RSM was used to compose the CCD for optimization of different reaction parameters. A quadratic model was found to be significant with the *p*-value. The synthesized nano-catalyst was characterized by XRD, SEM, EDX, TEM, and FT-IR techniques. Different analytical techniques were also used such as TLC, GC-MS, FT-IR, and NMR for biodiesel characterization and confirmation. The catalyst was successfully recovered and reused four times and exhibited good recyclability; after that, a considerable decrease was observed in biodiesel yield. Physicochemical characterizations of biodiesel were also studied, i.e., flash point (97 °C), density (0.825 48 kg/m3 at 40 °C), Kinematic viscosity (4.66 cSt), pour point (−10 °C), cloud point (−14 °C), sulfur content (0.00066 %wt),

and total acid number (0.182 mg KOH/g) agreed with the prescribed limits of ASTM D-951, ASTM D 6751, and EN-14214. The minimum sulfur content of 0.0006% was observed in the present study which confirms the environment-friendly nature of synthesized biodiesel. The experimental data best fitted with Pseudo first-order kinetics.

The overall study concludes that the *Brassica juncea* (L.) Czern. seed oil is a promising candidate for the biofuel industry, along with a green, clean, and cheap phyto-nano-catalyst. It also plays a very important role in the management of bio-waste and encourages researchers to focus on waste biomass-based energy rather than the use of primary energy sources. In this way, it provides a momentous opportunity for a circular bio-economy. It is recommended to check the efficiency of other metals and oxides after modification with different types of green substances. Advanced statistical techniques such as artificial neural networking (ANN) have to be used for the optimization of synthesized biodiesel. A detailed LCA study is the need of the hour to investigate the social, economic, and environmental impacts of these non-edible oil seeds. A detailed "exergoeconoenvironmental analysis" needs to be developed to better comprehend the energy conversion system concurrently from thermodynamic, economic, and environmental perspectives.

Supplementary Materials: The following supporting information can be downloaded at https://www.mdpi.com/article/10.3390/su141610188/s1, Figure S1. Schematic representation (upper), Pictorial presentation (lower) of biodiesel Synthesis from BJSO using Ni-TG nanocatalyst. Figure S2. GC Spectra of *Brassica juncea* (L.) Czern. Biodiesel. Figure S3. ^{1}H NMR Spectra of *Brassica juncea* (L.) Czern. Seed Oil (upper), *Brassica juncea* Biodiesel (lower). Figure S4. ^{13}C NMR Spectra of *Brassica juncea* (L.) Czern. seed Oil (upper), *Brassica juncea* Biodiesel (lower).

Author Contributions: M.A. (Mushtaq Ahmad) and M.T.A. designed the whole experiment and methodology. M.T.A. collected the seeds and performed the whole experiment. M.A. (Mushtaq Ahmad), M.A. (Maliha Asma), M.Z. and M.M. revised the whole experiment carefully to its present form and assisted with checking the consistency of data. S.S. drafted the manuscript with contribution from M.A.M., A.M. and M.A.K. All authors have read and agreed to the published version of the manuscript.

Funding: This research was funded by Taif University, Saudi Arabia (Project number-TURSP-2020/32) and HEC (SRGP-10767).

Institutional Review Board Statement: Not applicable.

Informed Consent Statement: Not applicable.

Data Availability Statement: Not applicable.

Acknowledgments: We are thankful to Taif University, Saudi Arabia (Project number-TURSP-2020/32) and HEC (SRGP-10767) for research support funding.

Conflicts of Interest: The authors declare no conflict of interest.

Abbreviations

Al_2O_3	Aluminum Oxide
ANN	Artificial Neural Networking
ANOVA	Analysis of Variance
ASTM	American Standards and Testing Materials
BJBD	*Brassica juncea* Biodiesel
BJSO	*Brassica juncea* seeds oil
C.V	Coefficient of Variation
CCD	Central Composite Design
DEE	Diethyl ether
DTA	Differential Thermal Analysis
EDX	Energy Dispersive X-ray

EI	Electron Impact
FAME	Fatty Acid Methyl Esters
FFA	Free Fatty Acid
FT-IR	Fourier Transform Infrared Spectroscopy
F-value	the Variance of group means
GCMS	Gas Chromatography Mass Spectroscopy
GHG	Green House Gas
JCPDS	Joint Committee on Powder Diffraction Standards
LPO	Lemon Peel Oil
$NiSO_4$	Nickle Sulfate
NMR	Nuclear Magnetic Resonance
p-value	Probability of Obtaining the result
R_f	Retention factor
RSM	Response Surface Methodology
RSM	Response Surface Methodology
SEM	Scanning Electron Microscopy
St.dev	Standard deviation
TEM	Transmission Electron Microscopy
TG	Tragacanth gum
TGS	Tragacanth gum solution
TLC	Thin Layer Chromatography
XRD	X-ray Diffraction

References

1. Singh, N.K.; Singh, Y.; Sharma, A. Optimization of biodiesel synthesis from Jojoba oil via supercritical methanol: A response surface methodology approach coupled with genetic algorithm. *Biomass Bioenergy* **2022**, *156*, 106332. [CrossRef]
2. Bakır, H.; Ağbulut, U.; Gürel, A.E.; Yıldız, G.; Güvenç, U.; Soudagar, M.E.M.; Hoang, A.T.; Deepanraj, B.; Saini, G.; Afzal, A. Forecasting of future greenhouse gas emission trajectory for India using energy and economic indexes with various metaheuristic algorithms. *J. Clean. Prod.* **2022**, *360*, 131946. [CrossRef]
3. Awang, M.S.N.; Zulkifli, N.W.M.; Abbas, M.M.; Zulkifli, S.A.; Kalam, M.A.; Yusoff, M.N.A.M.; Daud, W.M.A.W.; Ahmad, M.H. Effect of diesel-palm biodiesel fuel with plastic pyrolysis oil and waste cooking biodiesel on tribological characteristics of lubricating oil. *Alex. Eng. J.* **2022**, *61*, 7221–7231. [CrossRef]
4. Gurunathan, B.; Ravi, A. Process optimization and kinetics of biodiesel production from neem oil using copper doped zinc oxide heterogeneous nanocatalyst. *Bioresour. Technol.* **2015**, *190*, 424–428. [CrossRef] [PubMed]
5. Aghilinategh, M.; Barati, M.; Hamadanian, M. The modified supercritical media for one-pot biodiesel production from *Chlorella vulgaris* using photochemically-synthetized $SrTiO_3$ nanocatalyst. *Renew. Energy* **2020**, *160*, 176–184. [CrossRef]
6. Khan, I.U.; Haleem, A. A seed of Albizzia julibrissin wild plant as an efficient source for biodiesel production. *Biomass Bioenergy* **2022**, *158*, 106381. [CrossRef]
7. Mahlia, T.M.I.; Syazmi, Z.A.H.S.; Mofijur, M.; Abas, A.P.; Bilad, M.R.; Ong, H.C.; Silitonga, A.S. Patent landscape review on biodiesel production: Technology updates. *Renew. Sustain. Energy Rev.* **2020**, *118*, 109526. [CrossRef]
8. Zhang, Y.; Duan, L.; Esmaeili, H. A review on biodiesel production using various heterogeneous nanocatalysts: Operation mechanisms and performances. *Biomass Bioenergy* **2022**, *158*, 106356. [CrossRef]
9. Yusuf, A.A.; Ampah, J.D.; Soudagar, M.E.M.; Veza, I.; Kingsley, U.; Afrane, S.; Jin, C.; Liu, H.; Elfasakhany, A.; Buyondo, K.A. Effects of hybrid nanoparticle additives in n-butanol/waste plastic oil/diesel blends on combustion, particulate and gaseous emissions from diesel engine evaluated with entropy-weighted PROMETHEE II and TOPSIS: Environmental and health risks of plastic waste. *Energy Convers. Manag.* **2022**, *264*, 115758. [CrossRef]
10. Soudagar, M.E.M.; Nik-Ghazali, N.N.; Kalam, M.A.; Badruddin, I.A.; Banapurmath, N.R.; Ali, M.A.B.; Kamangar, S.; Cho, H.M.; Akram, N. An investigation on the influence of aluminium oxide nano-additive and honge oil methyl ester on engine performance, combustion and emission characteristics. *Renew. Energy* **2020**, *146*, 2291–2307. [CrossRef]
11. Raju, V.D.; Soudagar, M.E.M.; Venu, H.; Nair, J.N.; Reddy, M.S.; Reddy, J.S.; Rao, T.S.; Khan, T.M.Y.; Ismail, K.A.; Elfasakhany, A. Experimental assessment of diverse diesel engine characteristics fueled with an oxygenated fuel added lemon peel biodiesel blends. *Fuel* **2022**, *324*, 124529. [CrossRef]
12. Fadhil, A.B.; Nayyef, A.W.; Al-Layla, N.M. Biodiesel production from nonedible feedstock, radish seed oil by cosolvent method at room temperature: Evaluation and analysis of biodiesel. *Energy Sources Part A Recovery Util. Environ. Eff.* **2020**, *42*, 1891–1901. [CrossRef]

13. Fizal, A.N.S.; Hossain, M.S.; Zulkifli, M.; Khalil, N.A.; Hamid, H.A.; Yahaya, A.N.A. Implementation of the supercritical CO_2 technology for the extraction of candlenut oil as a promising feedstock for biodiesel production: Potential and limitations. *Int. J. Green Energy* **2021**, *19*, 72–83. [CrossRef]
14. Shaheen, A.; Sultana, S.; Lu, H.; Ahmad, M.; Asma, M.; Mahmood, T. Assessing the potential of different nanocomposite (MgO, Al_2O_3-CaO and TiO_2) for efficient conversion of *Silybum eburneum* seed oil to liquid biodiesel. *J. Mol. Liq.* **2018**, *249*, 511–521. [CrossRef]
15. Akhtar, M.T.; Ahmad, M.; Shaheen, A.; Zafar, M.; Ullah, R.; Asma, M.; Sultana, S.; Munir, M.; Rashid, N.; Malik, K.; et al. Comparative study of liquid biodiesel from sterculia foetida (bottle tree) using CuO-CeO_2 and Fe_2O_3 nano catalysts. *Front. Energy Res.* **2019**, *7*, 4. [CrossRef]
16. Munir, M.; Ahmad, M.; Saeed, M.; Waseem, A.; Nizami, A.S.; Sultana, S.; Zafar, M.; Rehan, M.; Srinivasan, G.R.; Ali, A.M.; et al. Biodiesel production from novel non-edible caper (*Capparis spinosa* L.) seeds oil employing Cu–Ni doped ZrO_2 catalyst. *Renew. Sustain. Energy Rev.* **2020**, *138*, 110558. [CrossRef]
17. Ali, L.H.; Fadhil, A.B. Biodiesel production from spent frying oil of fish via alkali-catalyzed transesterification. *Energy Sources Part A Recovery Util. Environ. Eff.* **2013**, *35*, 564–573. [CrossRef]
18. Altikriti, E.T.; Fadhil, A.B.; Dheyab, M.M. Two-step base catalyzed transesterification of chicken fat: Optimization of parameters. *Energy Sources Part A Recovery Util. Environ. Eff.* **2015**, *37*, 1861–1866. [CrossRef]
19. Fadhil, A.B.; Saeed, L.I. Sulfonated tea waste: A low-cost adsorbent for purification of biodiesel. *Int. J. Green Energy* **2016**, *13*, 110–118. [CrossRef]
20. Fadhil, A.B.; Nayyef, A.W.; Sedeeq, S.H. Valorization of mixed radish seed oil and *Prunus armeniaca* L. oil as a promising feedstock for biodiesel production: Evaluation and analysis of biodiesels. *Asia-Pac. J. Chem. Eng.* **2020**, *15*, e2390. [CrossRef]
21. Szollosi, R. (Ed.) Indian Mustard (*Brassica juncea* L.) Seeds in Health. In *Nuts and Seeds in Health and Disease Prevention*; Academic Press: Cambridge, MA, USA, 2011; pp. 671–676. [CrossRef]
22. Sateesh, K.A.; Yaliwal, V.S.; Soudagar, M.E.M.; Banapurmath, N.R.; Fayaz, H.; Safaei, M.R.; Elfasakhany, A.; El-seesy, A. Utilization of biodiesel/Al_2O_3 nanoparticles for combustion behavior enhancement of a diesel engine operated on dual fuel mode. *J. Therm. Anal. Calorim.* **2022**, *147*, 5897–5911. [CrossRef]
23. Zulqarnain; Mohd Yusoff, M.H.; Ayoub, M.; Ramzan, N.; Nazir, M.H.; Zahid, I.; Abbas, N.; Elboughdiri, N.; Mirza, C.R.; Butt, T.A. Overview of Feedstocks for Sustainable Biodiesel Production and Implementation of the Biodiesel Program in Pakistan. *ACS Omega* **2021**, *6*, 19099–19114. [CrossRef] [PubMed]
24. Abbaszaadeh, A.; Ghobadian, B.; Omidkhah, M.R.; Najafi, G. Current biodiesel production technologies: A comparative review. *Energy Convers. Manag.* **2012**, *63*, 138–148. [CrossRef]
25. Ewunie, G.A.; Morken, J.; Lekang, O.I.; Yigezu, Z.D. Factors affecting the potential of Jatropha curcas for sustainable biodiesel production: A critical review. *Renew. Sustain. Energy Rev.* **2021**, *137*, 110500. [CrossRef]
26. Elnajjar, E.; Al-Omari, S.A.B.; Selim, M.Y.E.; Purayil, S.T.P. CI engine performance and emissions with waste cooking oil biodiesel boosted with hydrogen supplement under different load and engine parameters. *Alex. Eng. J.* **2022**, *61*, 4793–4805. [CrossRef]
27. Ullah, H.; Nafees, M.; Iqbal, F.; Awan, S.; Shah, A.; Waseem, A. Adsorption Kinetics of Malachite green and Methylene blue from aqueous solutions using surfactant modified Organoclays. *Acta Chim. Slov.* **2017**, *64*, 449–460. [CrossRef] [PubMed]
28. Saeed, T.; Miah, M.J.; Majed, N.; Hasan, M.; Khan, T. Pollutant removal from landfill leachate employing two-stage constructed wetland mesocosms: Co-treatment with municipal sewage. *Environ. Sci. Pollut. Res.* **2020**, *27*, 28316–28332. [CrossRef] [PubMed]
29. Naveenkumar, R.; Baskar, G. Optimization and techno-economic analysis of biodiesel production from *Calophyllum inophyllum* oil using heterogeneous nanocatalyst. *Bioresour. Technol.* **2020**, *315*, 123852. [CrossRef] [PubMed]
30. Harun, F.W.; Jihadi, N.I.M.; Ramli, S.; Hassan, N.R.A.; Zubir, N.A.M. Esterification of oleic acid with alcohols over Cu-MMT K10 and Fe-MMT K10 as acid catalysts. *AIP Conf Proc.* **2018**, *1972*, 030025. [CrossRef]
31. Ingle, A.P.; Chandel, A.K.; Philippini, R.; Martiniano, S.E.; da Silva, S.S. Advances in nanocatalysts mediated biodiesel production: A critical appraisal. *Symmetry* **2020**, *12*, 256. [CrossRef]
32. Mallakpour, S.; Ramezanzade, V. Tragacanth gum mediated green fabrication of mesoporous titania nanomaterials: Application in photocatalytic degradation of crystal violet. *J. Environ. Manag.* **2021**, *291*, 112680. [CrossRef]
33. Andrade, M.R.d.; Silva, C.B.; Costa, T.K.O.; Neto, E.L.d.; Lavoie, J.M. An experimental investigation on the effect of surfactant for the transesterification of soybean oil over eggshell-derived CaO catalysts. *Energy Convers. Manag. X* **2021**, *11*, 100094. [CrossRef]
34. Dawood, S.; Ahmad, M.; Ullah, K.; Zafar, M.; Khan, K. Synthesis and characterization of methyl esters from non-edible plant species yellow oleander oil, using magnesium oxide (MgO) nano-catalyst. *Mater. Res. Bull.* **2018**, *101*, 371–379. [CrossRef]
35. Nagaraja, K.; Rao, K.M.; Reddy, G.V.; Rao, K.K. Tragacanth gum-based multifunctional hydrogels and green synthesis of their silver nanocomposites for drug delivery and inactivation of multidrug resistant bacteria. *Int. J. Biol. Macromol.* **2021**, *174*, 502–511. [CrossRef] [PubMed]
36. Padil, V.V.; Wacławek, S.; Černík, M.; Varma, R.S. Tree gum-based renewable materials: Sustainable applications in nanotechnology, biomedical and environmental fields. *Biotechnol. Adv.* **2018**, *36*, 1984–2016. [CrossRef]
37. Munir, M.; Ahmad, M.; Saeed, M.; Waseem, A.; Rehan, M.; Nizami, A.S.; Zafar, M.; Arshad, M.; Sultana, S. Sustainable production of bioenergy from novel non-edible seed oil (*Prunus cerasoides*) using bimetallic impregnated montmorillonite clay catalyst. *Renew. Sustain. Energy Rev.* **2019**, *109*, 321–332. [CrossRef]

38. Souza, M.C.G.; de Oliveira, M.F.; Vieira, A.T.; de Faria, A.M.; Batista, A.C.F. Methylic and ethylic biodiesel production from crambe oil (*Crambe abyssinica*): New aspects for yield and oxidative stability. *Renew. Energy* **2021**, *163*, 368–374. [CrossRef]
39. Rozina; Ahmad, M.; Asif, S.; Klemeš, J.J.; Mubashir, M.; Bokhari, A.; Sultana, S.; Mukhtar, A.; Zafar, M.; Bazmi, A.A.; et al. Conversion of the toxic and hazardous *Zanthoxylum armatum* seed oil into methyl ester using green and recyclable silver oxide nanoparticles. *Fuel* **2022**, *310*, 122296. [CrossRef]
40. Yadav, M.; Sharma, Y.C. Process optimization and catalyst poisoning study of biodiesel production from kusum oil using potassium aluminum oxide as efficient and reusable heterogeneous catalyst. *J. Clean. Prod.* **2018**, *199*, 593–602. [CrossRef]
41. Sidik, S.M.; Triwahyono, S.; Jalil, A.A.; Majid, Z.A.; Salamun, N.; Talib, N.B.; Abdullah, T.A.T. CO_2 reforming of CH_4 over Ni–Co/MSN for syngas production: Role of Co as a binder and optimization using RSM. *Chem. Eng. J.* **2016**, *295*, 1–10. [CrossRef]
42. Marzouk, N.M.; el Naga, A.O.A.; Younis, S.A.; Shaban, S.A.; el Torgoman, A.M.; el Kady, F.Y. Process optimization of biodiesel production via esterification of oleic acid using sulfonated hierarchical mesoporous ZSM-5 as an efficient heterogeneous catalyst. *J. Environ. Chem. Eng.* **2021**, *9*, 105035. [CrossRef]
43. Chumuang, N.; Punsuvon, V. Response surface methodology for biodiesel production using calcium methoxide catalyst assisted with tetrahydrofuran as cosolvent. *J. Chem.* **2017**, *2017*, 4190818. [CrossRef]
44. Dantas, J.; Leal, E.; Cornejo, D.R.; Kiminami, R.H.G.A.; Costa, A.C.F.M. Biodiesel production evaluating the use and reuse of magnetic nanocatalysts $Ni_{0.5}Zn_{0.5}Fe_2O_4$ synthesized in pilot-scale. *Arab. J. Chem.* **2020**, *13*, 3026–3042. [CrossRef]
45. Khan, I.U.; Yan, Z.; Chen, J. Optimization, transesterification and analytical study of Rhus typhina non-edible seed oil as biodiesel production. *Energies* **2019**, *12*, 4290. [CrossRef]
46. Gousi, M.; Andriopoulou, C.; Bourikas, K.; Ladas, S.; Sotiriou, M.; Kordulis, C.; Lycourghiotis, A. Green diesel production over nickel-alumina coprecipitated catalysts. *Appl. Catal. A Gen.* **2017**, *536*, 45–56. [CrossRef]
47. Dawood, S.; Koyande, A.K.; Ahmad, M.; Mubashir, M.; Asif, S.; Klemeš, J.J.; Bokhari, A.; Saqib, S.; Lee, M.; Qyyum, M.A.; et al. Synthesis of biodiesel from non-edible (*Brachychiton populneus*) oil in the presence of nickel oxide nanocatalyst: Parametric and optimisation studies. *Chemosphere* **2021**, *278*, 130469. [CrossRef]
48. Sangeetha, G.; Rajeshwari, S.; Venckatesh, R. Green synthesis of zinc oxide nanoparticles by aloe barbadensis miller leaf extract: Structure and optical properties. *Mater. Res. Bull.* **2011**, *46*, 2560–2566. [CrossRef]
49. Booramurthy, V.K.; Kasimani, R.; Pandian, S. Biodiesel Production from Tannery Waste using a Nano Catalyst (Ferric-Manganese Doped Sulphated Zirconia). *Energy Sources Part A Recovery Util. Environ. Eff.* **2019**, *44*, 1092–1104. [CrossRef]
50. Kora, A.J.; Rastogi, L. Green synthesis of palladium nanoparticles using gum ghatti (*Anogeissus latifolia*) and its application as an antioxidant and catalyst. *Arab. J. Chem.* **2018**, *11*, 1097–1106. [CrossRef]
51. Tiwari, M.S.; Gawade, A.B.; Yadav, G.D. Magnetically separable sulfated zirconia as highly active acidic catalysts for selective synthesis of ethyl levulinate from furfuryl alcohol. *Green Chem.* **2017**, *19*, 963–976. [CrossRef]
52. Qu, T.; Niu, S.; Zhang, X.; Han, K.; Lu, C. Preparation of calcium modified Zn-Ce/Al_2O_3 heterogeneous catalyst for biodiesel production through transesterification of palm oil with methanol optimized by response surface methodology. *Fuel* **2021**, *284*, 118986. [CrossRef]
53. Garole, V.J.; Choudhary, B.C.; Tetgure, S.R.; Garole, D.J.; Borse, A.U. Palladium nanocatalyst: Green synthesis, characterization, and catalytic application. *Int. J. Environ. Sci. Technol.* **2019**, *16*, 7885–7892. [CrossRef]
54. Mansir, N.; Teo, S.H.; Rashid, U.; Taufiq-Yap, Y.H. Efficient waste Gallus domesticus shell derived calcium-based catalyst for biodiesel production. *Fuel* **2018**, *211*, 67–75. [CrossRef]
55. Loy, A.C.M.; Quitain, A.T.; Lam, M.K.; Yusup, S.; Sasaki, M.; Kida, T. Development of high microwave-absorptive bifunctional graphene oxide-based catalyst for biodiesel production. *Energy Convers. Manag.* **2019**, *180*, 1013–1025. [CrossRef]
56. Omar, W.N.N.W.; Amin, N.A.S. Optimization of heterogeneous biodiesel production from waste cooking palm oil via response surface methodology. *Biomass Bioenergy* **2011**, *35*, 1329–1338. [CrossRef]
57. Asif, S.; Ahmad, M.; Bokhari, A.; Chuah, L.F.; Klemes, J.J.; Akbar, M.M.; Sultana, S.; Yusup, S. Methyl ester synthesis of *Pistacia khinjuk* seed oil by ultrasonic-assisted cavitation system. *Ind. Crop. Prod.* **2017**, *108*, 336–347. [CrossRef]
58. Park, Y.M.; Lee, J.Y.; Chung, S.H.; Park, I.S.; Lee, S.Y.; Kim, D.K.; Lee, J.S.; Lee, K.Y. Esterification of used vegetable oils using the heterogeneous WO_3/ZrO_2 catalyst for production of biodiesel. *Bioresour. Technol.* **2010**, *101*, S59–S61. [CrossRef] [PubMed]
59. Elkelawy, M.; Bastawissi, H.A.E.; Esmaeil, K.K.; Radwan, A.M.; Panchal, H.; Sadasivuni, K.K.; Suresh, M.; Israr, M. Maximization of biodiesel production from sunflower and soybean oils and prediction of diesel engine performance and emission characteristics through response surface methodology. *Fuel* **2020**, *266*, 117072. [CrossRef]
60. Rozina; Ahmad, M.; Zafar, M. Conversion of waste seed oil of Citrus aurantium into methyl ester via green and recyclable nanoparticles of zirconium oxide in the context of circular bioeconomy approach. *Waste Manag.* **2021**, *136*, 310–320. [CrossRef] [PubMed]
61. Olutoye, M.A.; Lee, S.C.; Hameed, B.H. Synthesis of fatty acid methyl ester from palm oil (*Elaeis guineensis*) with Ky (MgCa) 2xO3 as heterogeneous catalyst. *Bioresour. Technol.* **2011**, *102*, 10777–10783. [CrossRef]
62. Maulidiyah; Nurdin, M.; Fatma, F.; Natsir, M.; Wibowo, D. Characterization of methyl ester compound of biodiesel from industrial liquid waste of crude palm oil processing. *Anal. Chem. Res.* **2017**, *12*, 1–9. [CrossRef]
63. Rahman, M.A. Valorization of harmful algae E. compressa for biodiesel production in presence of chicken waste derived catalyst. *Renew. Energy* **2018**, *129*, 132–140. [CrossRef]

64. Borah, M.J.; Devi, A.; Borah, R.; Deka, D. Synthesis and application of Co doped ZnO as heterogeneous nanocatalyst for biodiesel production from non-edible oil. *Renew. Energy* **2019**, *133*, 512–519. [CrossRef]
65. Sokoto, M.A.; Hassan, L.G.; Dangoggo, S.M.; Ahmad, H.G.; Uba, A. Influence of fatty acid methyl esters on fuel properties of biodiesel produced from the seeds oil of *Curcubita pepo*. *Niger. J. Basic Appl. Sci.* **2011**, *19*, 81–86. [CrossRef]
66. Tariq, M.; Ali, S.; Ahmad, F.; Ahmad, M.; Zafar, M.; Khalid, N.; Khan, M.A. Identification, FT-IR, NMR (1H and 13C) and GC/MS studies of fatty acid methyl esters in biodiesel from rocket seed oil. *Fuel Process. Technol.* **2011**, *92*, 336–341. [CrossRef]
67. Guzatto, R.; Defferrari, D.; Reiznautt, Q.B.; Cadore, I.R.; Samios, D. Transesterification double step process modification for ethyl ester biodiesel production from vegetable and waste oils. *Fuel* **2012**, *92*, 197–203. [CrossRef]
68. Maneerung, T.; Kawi, S.; Dai, Y.; Wang, C.H. Sustainable biodiesel production via transesterification of waste cooking oil by using CaO catalysts prepared from chicken manure. *Energy Convers. Manag.* **2016**, *123*, 487–497. [CrossRef]
69. Krishnamurthy, K.N.; Sridhara, S.N.; Kumar, C.A. Optimization and kinetic study of biodiesel production from *Hydnocarpus wightiana* oil and dairy waste scum using snail shell CaO nano catalyst. *Renew. Energy* **2020**, *146*, 280–296. [CrossRef]